

*Supporting Information*

**Ambipolar Macrocycle Derived from Spiro-Xanthene and Carbazole:  
Synthesis, Structure-Property Relationships, Electronic Properties and  
Host-Guest Investigation**

<b>S.No</b>	<b>Table of contents</b>	<b>Page number</b>
01	Synthetic Methods	S3-S9
02	Additional spectroscopic data	S10-S15
03	Electrochemistry	S16-S17
04	Computational methods and techniques	S17-S24
05	Host-Guest analysis	S24-S27
06	SCLC measurements	S28-S29
07	NMR spectra	S30-S39
08	Mass data	S40-S43
09	References	S45

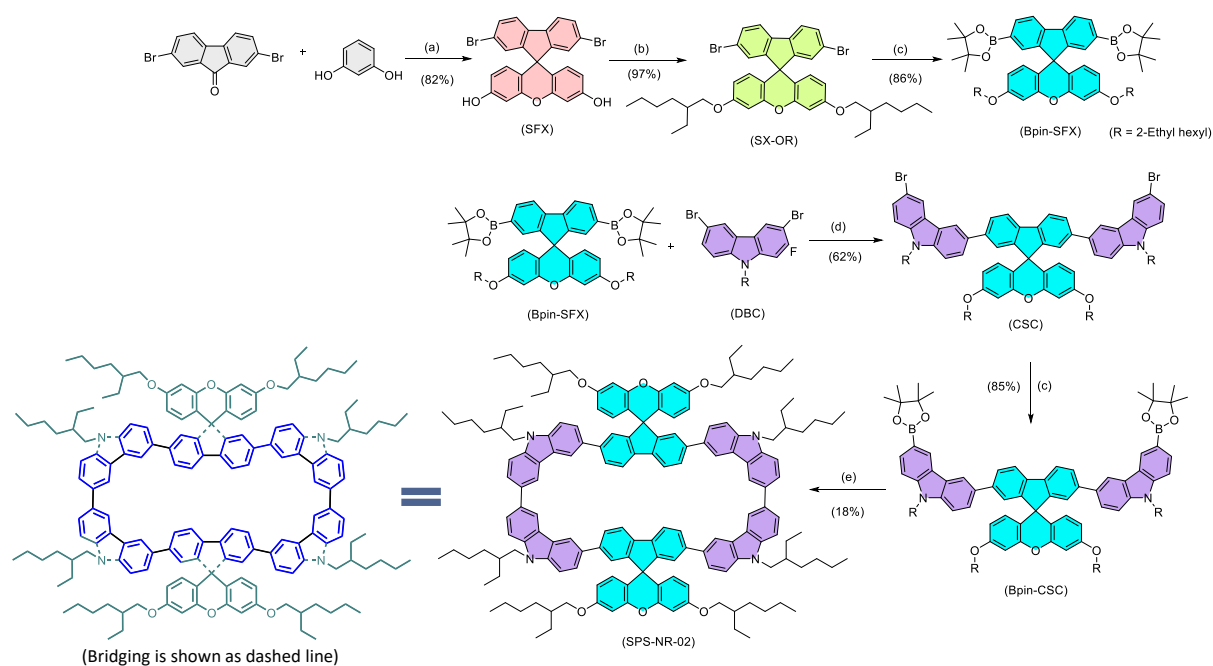
## 1. Synthetic methods:

### 1.1 General information:

All the reagents were purchased from commercial sources and used without further purification. Starting materials 2,7-dibromo-9-fluorenone, resorcinol and 2-ethylhexyl bromide was purchased from TCI. 2,7-dibromospiro[fluorene-9,9'-xanthene]-3',6'-diol (SFX) was synthesized following the reported procedure.<sup>[1]</sup> 3,6-dibromo carbazole and 3,6-dibromo-9-(2-ethylhexyl)-9H-carbazole were synthesized following the earlier synthetic protocol.<sup>[2]</sup> The solvents used for the reaction were distilled prior to use following standard distillation processes and stored over molecular sieves.<sup>[3]</sup> All the reactions were performed under Argon atmosphere. Column chromatography was performed using silica gel (100-200 mesh). Proton <sup>1</sup>H NMR were recorded on Bruker 400 MHz and 500 MHz instruments. Carbon <sup>13</sup>C NMR were recorded on Bruker 101MHz instrument. Tetramethyl silane (TMS) was used as the internal standard. Chemical shifts were given in parts per million (ppm) relative to residue protons (CDCl<sub>3</sub>: δ 7.26 for <sup>1</sup>H, δ 77.16 for <sup>13</sup>C). The abbreviations s, d, t, dd, m corresponds to multiplicities singlet, doublet, triplet, doublet of doublet and multiplet respectively. HRMS (ESI) were recorded on ORBITRAP mass analyzer (Thermo Scientific, Exploris 120). Matrix Assisted Laser Desorption Ionization (MALDI) mass spectra were recorded on Bruker Daltonics Autoflex Time of flight (TOF) equipment. Elemental analyses of C, H, N and O were determined with the instrument Elementar Vario EL III CHNS analyzer.

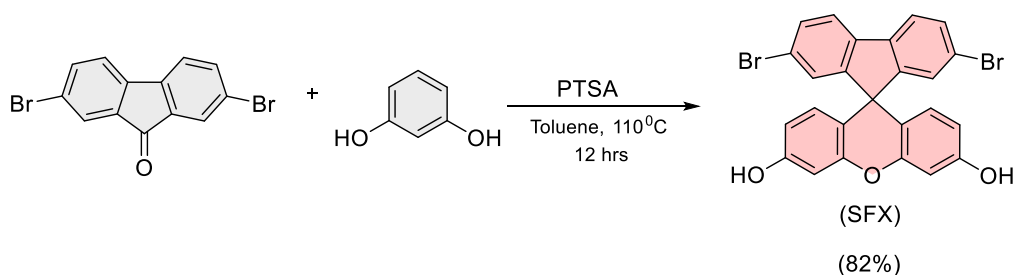
The steady state UV/vis and fluorescence spectroscopy were recorded using SHIMADZU UV-2600 and FL-1000 spectrophotometer respectively. All the solvents used to record the data are of HPLC grade. The absolute photoluminescence quantum yields were calculated using Edinburgh FLS1000 spectrophotometer using integrated sphere accessory. Fluorescence lifetime was measured by the method of time correlated single photon counting (TCSPC) technique recorded using HORIBA JOBIN YVON FLUORO-CUBE instrument. The electrochemical measurements were recorded in anhydrous DCM. A three-electrode system with glassy carbon as working electrode, Pt wire as counter electrode and Ag/AgNO<sub>3</sub> as reference electrode. Tetrabutylammonium hexafluorophosphate n-Bu<sub>4</sub>NPF<sub>6</sub> was used as the supporting electrolyte. The potential was calibrated against ferrocene/ferrocenium couple.

## Synthetic scheme:



**Scheme S1:** Synthetic route of SPS-NR-02. Reagents and conditions: (a) p-toluenesulfonic acid, toluene, 110°C, 12 hrs. (b) 2-ethylhexyl bromide, KOH, DMSO, RT, 8 hrs. (c) Bis(pinacolato)diboron, KOAc, 1,4-dioxane, 100°C, 24 hrs, (d)  $K_2CO_3$ ,  $Pd(PPh_3)_4$ ,  $H_2O$ , toluene, 110°C, 18 hrs. (e)  $KF$ ,  $B(OH)_3$ ,  $Pd(PPh_3)_2Cl_2$ , tetrahydrofuran,  $H_2O$  40°C, 24 hrs.

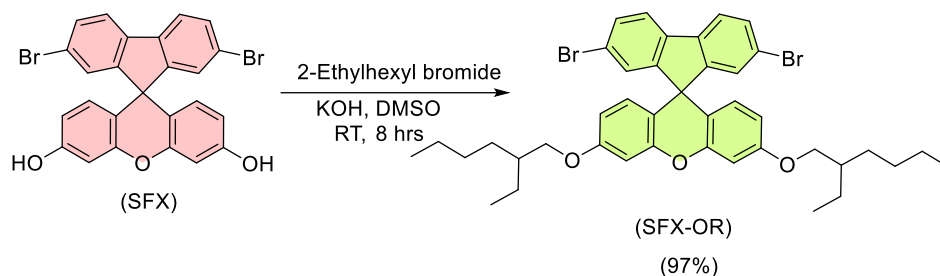
## 1.2 Synthesis of SFX:



2,7-dibromo fluorenone (600 mg, 1.78 mmol), resorcinol (782 mg, 7.10 mmol) was added to a 100 ml round bottom flask. Toluene (30 ml) was added and the solution was stirred for 15 min at room temperature. Then p-toluene sulfonic acid (33.8 mg, 0.178 mmol) was added and the reaction mixture was maintained at 110°C for 12 hrs. After completion of reaction, the round bottom flask was allowed to cool down to room temperature. Water (30 ml) was added and the mixture was stirred for 30 min. The solid was collected by filtration, washed with water and methanol (3 ml). The solid was dried overnight to obtain pale red solid with 82% yield (760

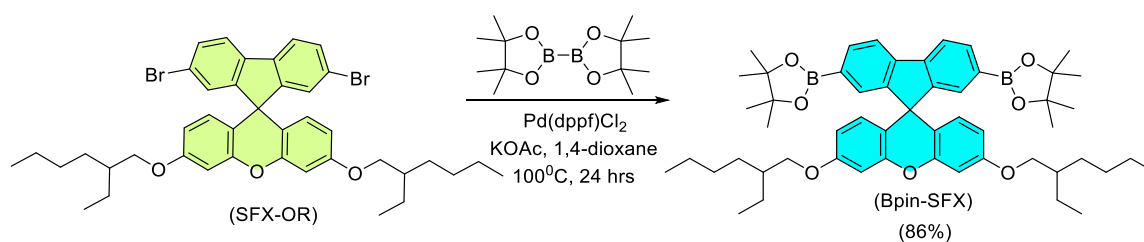
mg, 1.5 mmol).  $^1\text{H NMR}$  (400 MHz,  $\text{DMSO-d}_6$ )  $\delta$  9.79 (s, 1H), 7.99 (d,  $J = 8.2$  Hz, 1H), 7.63 (d,  $J = 8.1$  Hz, 1H), 7.19 (s, 1H), 6.67 (d,  $J = 1.7$  Hz, 1H), 6.37 (dd,  $J = 8.5, 1.8$  Hz, 1H), 6.13 (d,  $J = 8.5$  Hz, 1H).  $^{13}\text{C NMR}$  (101 MHz,  $\text{DMSO-d}_6$ )  $\delta$  158.2, 157.6, 151.7, 137.8, 131.6, 128.7, 128.3, 123.3, 122.1, 113.4, 112.4, 103.3, 53.4. Characterization details are in correlation with the reported literature.<sup>[1]</sup>

### 1.3 Synthesis of SFX-OR:



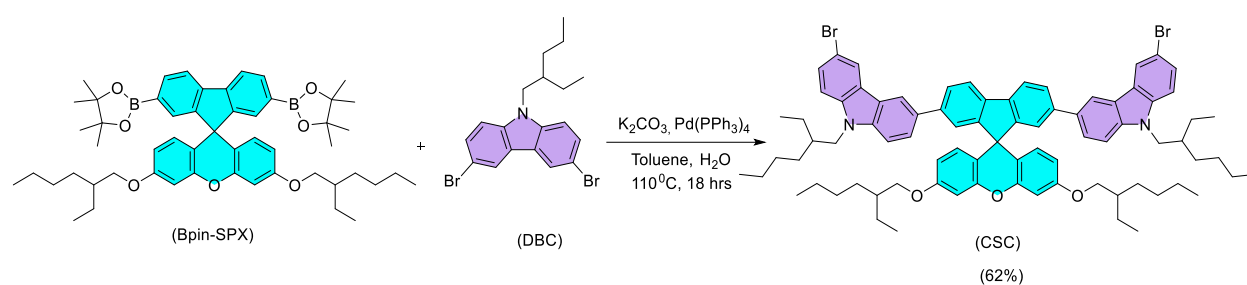
To an oven dried 100 ml round bottom flask SFX (500 mg, 0.958 mmol) and DMSO (15 ml) was added. After 15 min, KOH (537 mg, 9.58 mmol) was finely grinded and slowly added to the solution. 2-Ethylhexyl bromide (425 mg, 2.20 mmol) was added and it was maintained at room temperature for 8 hrs. The completion of reaction was checked using TLC and the DMSO solution was added to ice. It was extracted using DCM. The same procedure was repeated five times to remove DMSO completely. The organic phase was dried over  $\text{Na}_2\text{SO}_4$  and concentrated. The mixture was purified using Column chromatography (100-200 silica) using hexane as eluent. The final product was obtained as colourless solid with 97% yield.  $^1\text{H NMR}$  (400 MHz,  $\text{CDCl}_3$ )  $\delta$  7.59 (d,  $J = 8.1$  Hz, 2H), 7.46 (dd,  $J = 8.1, 1.8$  Hz, 2H), 7.23 (d,  $J = 1.7$  Hz, 2H), 6.73 (d,  $J = 2.5$  Hz, 2H), 6.40 (dd,  $J = 8.7, 2.5$  Hz, 2H), 6.24 (d,  $J = 8.7$  Hz, 2H), 3.83 (d,  $J = 5.7$  Hz, 4H), 1.71 (m, 2H), 1.52 – 1.30 (m, 16H), 0.92 (t,  $J = 7.6$  Hz, 12H).  $^{13}\text{C NMR}$  (101 MHz,  $\text{CDCl}_3$ )  $\delta$  159.6, 157.2, 151.9, 137.5, 131.1, 129.0, 128.6, 122.4, 121.3, 114.7, 111.4, 101.9, 70.6, 53.5, 39.3, 30.5, 29.1, 23.9, 23.1, 14.1, 11.1. HRMS (ESI)  $m/z$ :  $[\text{M}+\text{H}]^+$  calcd for  $\text{C}_{41}\text{H}_{47}\text{Br}_2\text{O}_3$  745.1892; found 745.1886. m.p.: 104-106°C.

### 1.4 Synthesis of Bpin-SFX:



SFX-OR (500 mg, 0.670 mmol) was added to an oven dried 100 ml round bottom flask. The RB was connected to high vacuum and evacuated for 15 min and refilled with N<sub>2</sub>. The procedure was repeated for three times. KOAc (850 mg, 3.35 mmol) and Bis(pinacolato)diboron (197 mmol, 2.01 mmol) was added and again the evacuation procedure was repeated twice. 1,4-dioxane (25ml) was added and the solution was degassed with N<sub>2</sub> for 30 min. Finally, Pd(dppf)Cl<sub>2</sub>.CH<sub>2</sub>Cl<sub>2</sub> (27.3 mg, 0.033 mmol) was added and degassed for 15 min. The dark red solution was heated to 100 °C and maintained for 24 hrs. After confirming the complete consumption of starting material using TLC, dioxane was removed using rotatory evaporator. DCM was added to the crude mixture and the organic layer was washed with brine solution (3-times) and finally with water. The organic layer was dried over anhydrous Na<sub>2</sub>SO<sub>4</sub> and concentrated. The crude mixture was purified using column chromatography (100-200 silica mesh) using 5% ethyl acetate in hexane as eluent to obtain the target product as colourless solid with 86% yield (480 mg, 0.58 mmol). <sup>1</sup>H NMR (400 MHz, CDCl<sub>3</sub>) δ 7.80 (q, *J* = 7.6 Hz, 2H), 7.51 (s, 2H), 6.70 (d, *J* = 2.5 Hz, 2H), 6.32 (dd, *J* = 8.7, 2.5 Hz, 2H), 6.19 (d, *J* = 8.7 Hz, 2H), 3.82 (d, *J* = 5.7 Hz, 4H), 1.69 (m, 2H), 1.51 – 1.33 (m, 16H), 1.28 (s, 24H), 0.92 (t, *J* = 7.8 Hz, 12H). <sup>13</sup>C NMR (101 MHz, CDCl<sub>3</sub>) δ 159.0, 155.9, 151.9, 142.2, 134.4, 132.0, 129.3, 119.4, 115.8, 111.1, 101.5, 83.8, 83.5, 70.6, 53.2, 39.3, 29.1, 25.1, 24.9, 23.9, 23.1, 14.1, 11.1. HRMS (ESI) *m/z*: [M+H]<sup>+</sup> calcd for C<sub>53</sub>H<sub>71</sub>B<sub>2</sub>O<sub>7</sub> 841.5385; found 841.5354. m.p.: 118-121°C.

### 1.5 Synthesis of CSC:

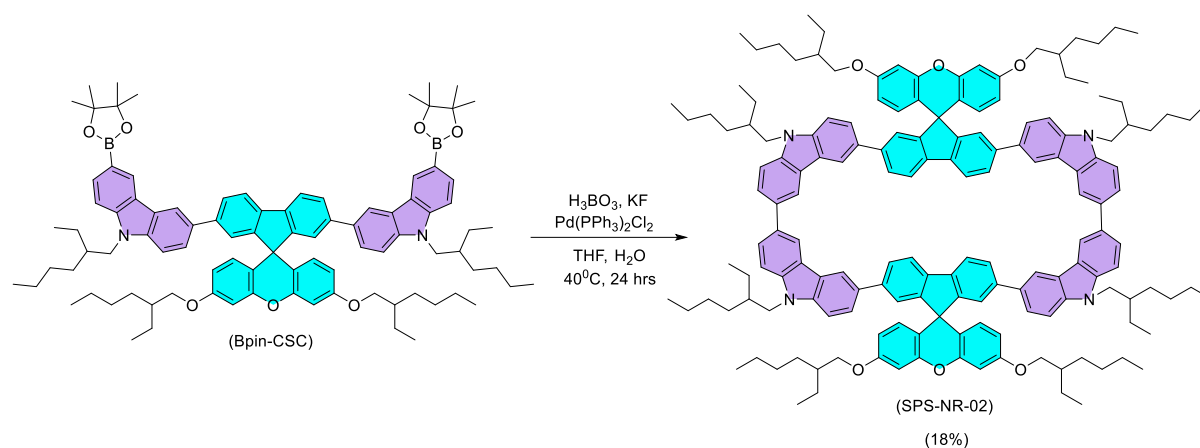


The synthesized Bpin-SFX (200 mg, 0.238 mmol) and 3,6-dibromo-9-(2-ethylhexyl)-9H-carbazole (DBC) (520 mg, 1.19 mmol) were added to an oven dried 50 ml round bottom flask. Dry toluene (20 ml) was added and the reaction mixture was stirred at room temperature while purging N<sub>2</sub> gas for 20-30 min. K<sub>2</sub>CO<sub>3</sub> (98 mg, 0.714 mmol) was dissolved in H<sub>2</sub>O (2 ml) and added to the reaction mixture using a syringe. The purging was continued for another 15 min. Finally, Pd(PPh<sub>3</sub>)<sub>4</sub> (9 mg, 0.012 mmol) was added and maintained at 110 °C for 18 hrs. The progression of the reaction was monitored using TLC. After the complete consumption of starting material, toluene was removed and DCM was added. The organic layer was washed



2H), 8.31 (d,  $J = 1.5$  Hz, 2H), 7.90 (d,  $J = 8.1$  Hz, 4H), 7.74 (dd,  $J = 7.9, 1.6$  Hz, 2H), 7.64 (dd,  $J = 8.5, 1.7$  Hz, 2H), 7.49 (d,  $J = 1.3$  Hz, 2H), 7.36 (d,  $J = 8.4$  Hz, 4H), 6.80 (d,  $J = 2.4$  Hz, 2H), 6.48 (d,  $J = 8.7$  Hz, 2H), 6.41 (dd,  $J = 8.8, 2.4$  Hz, 2H), 4.16 (d,  $J = 3.6$  Hz, 4H), 3.84 (d,  $J = 5.8$  Hz, 4H), 2.03 (m, 2H), 1.69 (m, 2H), 1.40 (s, 24H), 1.29 (m, 32H), 0.90 (m, 24H).  $^{13}\text{C}$  NMR (101 MHz,  $\text{CDCl}_3$ )  $\delta$  159.2, 156.9, 152.1, 143.5, 141.8, 140.4, 137.9, 132.5, 132.2, 129.1, 127.9, 126.7, 125.2, 124.3, 123.5, 122.7, 120.1, 118.8, 116.8, 111.1, 109.1, 108.5, 101.9, 83.6, 83.5, 70.5, 53.7, 47.5, 39.4, 31.0, 30.6, 29.1, 28.8, 25.1, 25.0, 24.6, 24.4, 23.9, 23.1, 14.1, 11.2, 10.9. HRMS (ESI)  $m/z$ :  $[\text{M}+\text{H}]^+$  calcd for  $\text{C}_{93}\text{H}_{117}\text{B}_2\text{N}_2\text{O}_7$  1395.9046; found 1395.9008. m.p.: 159-161°C.

### 1.7 Synthesis of SPS-NR-02:



The final macrocycle was prepared following the reaction protocol developed by Jasti et.al.<sup>4</sup> To a wide neck 500 ml reagent bottle was added Bpin-CSC (200 mg, 143  $\mu\text{mol}$ ), boric acid (44.3 mg, 717  $\mu\text{mol}$ ) and  $\text{Pd}(\text{PPh}_3)_2\text{Cl}_2$  (20.1 mg, 28.7  $\mu\text{mol}$ ). 300 ml THF was added and the reaction mixture was maintained at room temperature for 15 min. KF (33.3 mg, 573  $\mu\text{mol}$ ) was added followed by the addition of water (30 ml) and maintained for 10 min. The colour of the reaction mixture changed from pale yellow to yellow during the time. It was heated to 40 °C and maintained for 24 hours leaving it open to the atmosphere. The completion of reaction is checked by TLC and THF was removed. The crude mixture was dissolved in DCM and washed with brine solution twice and with water. The organic layer was dried over anhydrous  $\text{Na}_2\text{SO}_4$  and concentrated. It was purified by column chromatography 1:4 (V/V) chloroform: hexane followed by trituration using pentane and methanol. The final product was oven dried and was obtained as beige solid with 18% yield (59 mg, 26  $\mu\text{mol}$ ).  $^1\text{H}$  NMR (400 MHz,  $\text{CDCl}_3$ )  $\delta$  8.52 – 8.02 (m, 8H), 7.91 – 7.32 (m, 28H), 6.78 (s, 4H), 6.45 (dd,  $J = 28.4, 7.4$  Hz, 8H), 4.16 (d,  $J = 14.6$  Hz, 8H), 3.82 (s, 8H), 2.08 (d,  $J = 23.6$  Hz, 1H), 2.15 – 1.96 (m, 4H), 1.74 – 1.62 (m, 4H), 1.50 – 1.23 (m, 64H), 0.99 – 0.77 (m, 48H).  $^{13}\text{C}$  NMR (101 MHz,  $\text{CDCl}_3$ )  $\delta$  159.2, 156.8,



152.2, 142.1, 141.3, 140.9, 140.4, 137.9, 133.4, 132.0, 130.5, 129.1, 127.3, 126.8, 125.7, 125.3, 124.3, 123.6, 123.5, 123.2, 123.0, 120.5, 120.1, 118.8, 118.7, 116.9, 111.1, 109.3, 109.1, 101.8, 70.6, 53.8, 47.6, 39.4, 39.4, 31.0, 30.5, 29.1, 28.9, 24.4, 23.9, 23.1, 14.1, 11.1, 10.9. MALDI-TOF m/z calculated for  $C_{162}H_{184}N_4O_6$  2282.42 found 2282.42. Elemental analysis calcd: C-85.18%, H-8.16%, N-2.45%, O-4.20%; found: C-85.11%, H-8.13%, N-2.37%, O-4.16%. m.p.: 190-193°C.

## 2. Additional spectroscopic data:

### 2.1 Molar Absorption Coefficient calculation:

Molar absorption coefficients ( $\epsilon$ ) were calculated using UV-vis absorption spectroscopy. Absorbance ( $< 0.1A$ ) of samples of different concentrations were recorded. The slope of the linear plot of absorbance vs concentration was calculated. The experiment was repeated thrice and the mean absorption coefficient value was noted down.

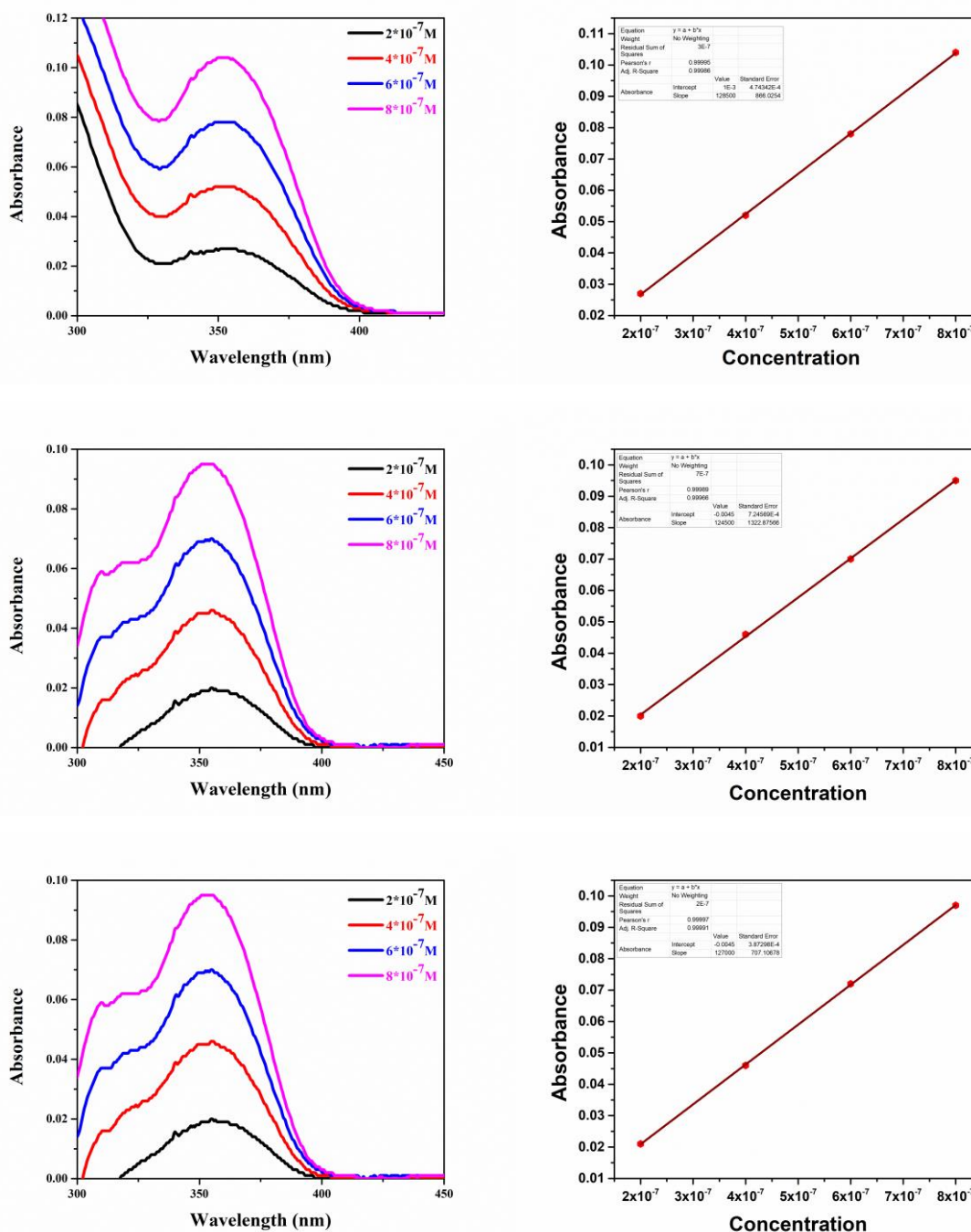


**Figure S1:** Absorption spectra of SPS-NR-02 in toluene (left) and linear fit of absorbance (right) at  $\lambda_{\max}$  as a function of concentration.

Concentration ( $\times 10^{-7}\text{M}$ )	Absorbance at $\lambda_{\text{max}}$ Trial-1	Absorbance at $\lambda_{\text{max}}$ Trial-2	Absorbance at $\lambda_{\text{max}}$ Trial-3
2	0.027	0.021	0.021
4	0.052	0.046	0.046
6	0.078	0.071	0.072
8	0.104	0.095	0.097

**Table S1:** Absorbance at  $\lambda_{\text{max}}$  for different concentrations.

	Slope ( $\times 10^5$ )	Average ( $\times 10^5$ )
Trial-1	1.28	1.26
Trial-2	1.24	
Trial-3	1.27	

**Table S2:** Molar absorption coefficient calculated using slope of linear plot.

## 2.2 Solvatochromism:

Absorption and emission spectra were recorded in different solvents of increasing polarity to understand the effect of solvent polarity on photophysical properties.

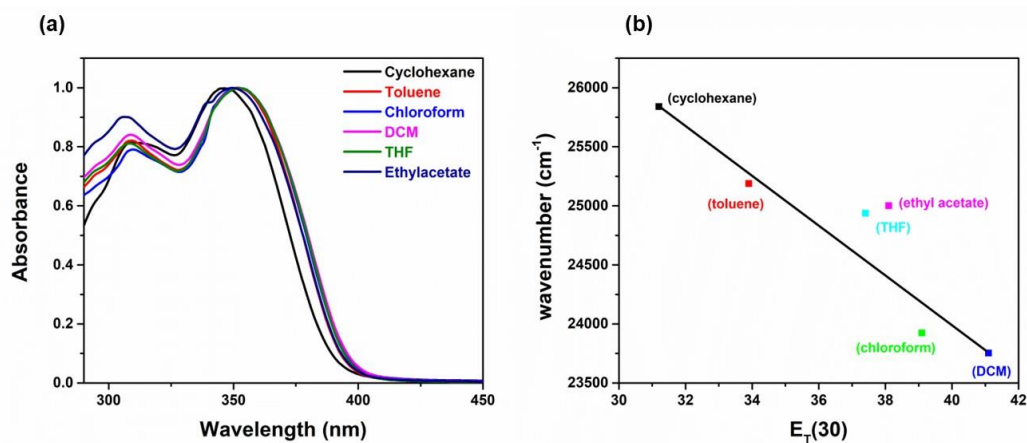


**Figure S2:** (a) Absorption spectra of SPS-NR-02 recorded in different solvents. (b) Plot of emission maxima (wavenumber) of SPS-NR-02 in various solvents against  $E_T(30)$ .

<b>Solvent</b>	$\lambda_{\max}$ (nm)	$\lambda_{\text{ems}}$ (nm)	<b>Stokes shift (nm)</b>	<b>E<sub>T</sub>(30)</b>
Cyclohexane	345	387	42	31.2
Toluene	351	397	46	33.9
THF	353	401	48	37.4
Ethyl acetate	349	400	51	38.1
Chloroform	351	418	67	39.1
DCM	351	421	70	41.1

**Table S3:** Absorption and emission maximal wavelengths of SPS-NR-02 in various solvents.

<b>Molecule</b>	$\lambda_{\max}$ (nm)	$\lambda_{\text{ems}}$ (nm)	<b>Stokes shift</b> (nm)	<b>HOMO</b> (eV)	<b>LUMO</b> (eV)	<b>Band gap</b> (eV)
SPS-NR-02 (experimental)	351	397	46	-5.17	-3.7	1.47
SPS-NR-02 (DFT)	356	380	44	-5.3	-1.0	4.3

**Table S4:** Experimental and calculated photophysical properties of stable conformer SPS-NR-02 at SRSH-LC- $\omega$ HPBE/6-31G(d,p) level of theory using PCM solvent model with toluene.

### 2.3 CIE Colour Coordinates:

Fluorescence spectroscopy analysis of macrocycle SPS-NR-02 resulted in deep-blue emission with CIE colour coordinates  $CIE_{[x,y]} = [0.16, 0.041]$  in toluene. As can be seen from Figure S3 the CIE colour coordinates are almost identical in all the analysed solvents.

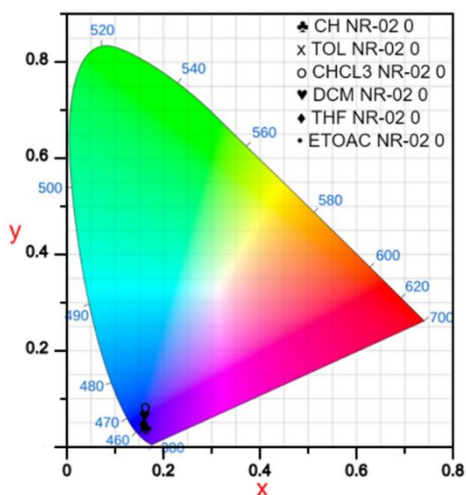


**Figure S3:** CIE chromatograph of SPS-NR-02 in different solvents.

### 2.4 Fluorescence lifetime measurements:

The time-resolved photoluminescence decay (TRPL) of SPS-NR-02 is recorded in different solvents. Fluorescence lifetime of the compound was measured by the method of time correlated single photon counting (TCSPC) technique recorded using HORIBA JOBIN YVON FLUORO-CUBE instrument. The sample was excited using a picosecond diode laser of 300 nm and the fluorescence signal at 410 nm was recorded. The slit width was 8 nm. The data was fitted using Datastation V2.6 software. Irrespective of the solvent polarity, all decay profiles were well fitted into bi-exponential decay. Convolution analysis gave a satisfactory bi-exponential fitting as indicated by  $\chi^2$  values. Fluorescence lifetimes were calculated by fitting the fluorescence decay into a two-component exponential curve using the equation  $F(t) = \alpha_1 e^{-t/\tau_1} + \alpha_2 e^{-t/\tau_2} + C$  where  $F(t)$  represents fluorescence intensity as function of time,  $\tau_1$  and  $\tau_2$  represents short and long fluorescence lifetimes respectively and  $\alpha_1, \alpha_2$  represents contribution from each life-time component.  $\tau_{avg}$  is calculated using the formula  $\langle \tau \rangle = \frac{\sum \alpha_i t_i^2}{\sum \alpha_i t_i}$ . Radiative rate constant ( $k_r$ ) and non-radiative rate constant ( $k_{nr}$ ) are calculated using the

values obtained from PLQY and  $\tau_{avg}$  by substituting in the equation  $k_r = \frac{PLQY}{\langle\tau\rangle}$  and  $k_{nr} = \frac{1-PLQY}{\langle\tau\rangle}$ .

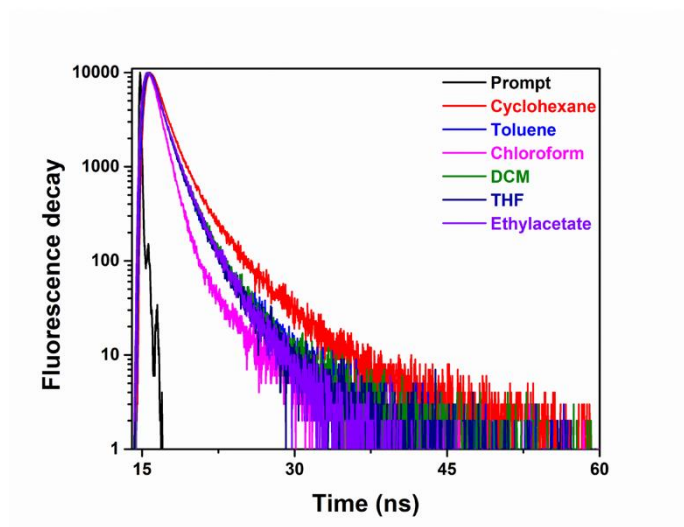


**Figure S4:** Fluorescence lifetime decay patterns of SPS-NR-02 in different solvents.

Solvent	$\tau_1$ (ns)	$\tau_2$ (ns)	$\alpha_1$ (%)	$\alpha_2$ (%)	$\langle\tau\rangle$ (ns)	$\chi^2$
Cyclohexane	1.170	3.747	77.92	22.08	2.396	1.121
Toluene	1.029	2.913	82.53	17.47	1.733	1.001
Chloroform	0.880	3.768	95.32	04.68	1.382	0.971
DCM	1.119	2.952	83.73	16.27	1.740	0.953
THF	1.107	2.859	84.92	15.08	1.658	0.949
Ethyl acetate	1.126	2.587	80.74	19.26	1.653	0.961

**Table S5:** Time resolved data of SPS-NR-02 in different solvents.

### 2.5 Lippert-Mataga Solvatochromism Measurements:

The solvent dependency of spectral shifts is described using Lippert-Mataga equation 1. Plotting Stokes shift as a function of orientation polarizability of solvents gives the Lippert-Mataga plot (fig S5).

$$\Delta\nu = \frac{2}{hc} \Delta f \frac{(\mu_E - \mu_G)^2}{a^3} + \text{constant} \dots \dots \dots 1$$

$$\text{Where } \Delta f = \frac{\epsilon - 1}{2\epsilon + 1} + \frac{\eta^2 - 1}{2\eta^2 + 1}$$

Where  $\Delta\nu$  is the Stokes shift,  $h$  is the Planck's constant,  $c$  is the velocity of light in vacuum,  $a$  is the Onsager radius of the cavity in which the molecule resides,  $\mu_E$  and  $\mu_G$  are the dipole moments of the excited and ground states respectively,  $\epsilon$  is the dielectric constant of the solvent,  $\eta$  is the refractive index of solvent and  $\Delta f$  is the orientation polarizability. The emission maxima redshifted from cyclohexane to DCM and then blue shifted for THF and ethyl acetate. As shown in fig S5 the plot of  $\Delta f$  against stokes shift is linear with a slope =  $2476.6 \text{ cm}^{-1}$ , intercept =  $4199 \text{ cm}^{-1}$ , Pearson's  $r = 0.97778$  and correlation coefficient  $R^2 = 0.95606$ .

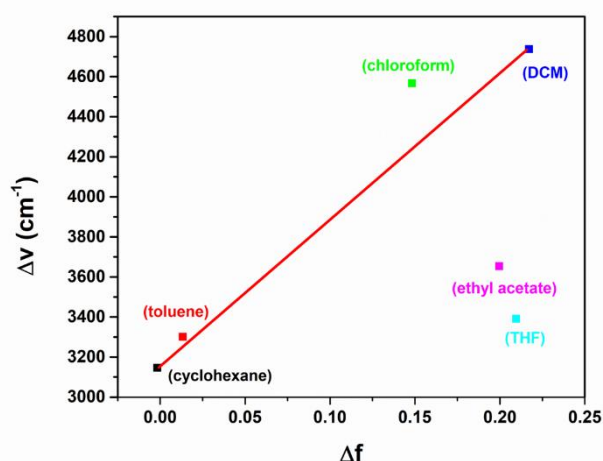


**Figure S5:** Lippert-Mataga formalism linear fit for SPS-NR-02 in different solvents.

Solvent	$\nu_{\text{abs}} \text{ (cm}^{-1}\text{)}$	$\nu_{\text{em}} \text{ (cm}^{-1}\text{)}$	$\Delta\nu \text{ (cm}^{-1}\text{)}$	$\Delta f$
Cyclohexane	28985.5	25839.8	3145.7	-0.00165
Toluene	28490.1	25188.9	3301.2	0.01324
Chloroform	28490.1	23923.4	4566.7	0.148295
DCM	28490.1	23752.9	4737.2	0.217137
THF	28328.6	24937.6	3391.0	0.209572
Ethyl acetate	28653.3	25000.0	3653.3	0.199635

**Table S6:** Lippert-Mataga formalism calculation of SPS-NR-02 in different solvents.

## Electrochemistry:

Electrochemistry experiments were performed using dichloromethane which was distilled prior to use. The experiments were conducted under Ar atmosphere. Platinum (Pt) disc electrode (diameter 1m) was used as a working electrode, reference electrode was a silver wire in 0.1 M AgNO<sub>3</sub> solution and carbon rod was used as a counter electrode. Tetra butyl ammonium hexafluorophosphate (Bu<sub>4</sub>NPF<sub>6</sub>) (0.2 M) was used as the electrolyte and ferrocene was added to the electrolyte solution. The oxidation and reduction potentials are referenced against ferrocene/ferrocenium (Fc/Fc<sup>+</sup>) couple. The three-electrode system was connected to the potentiostat and monitored using software at a sweep rate of 50 mV/s. As mentioned in the main text, SPS-NR-02 has one reversible and one quasi-reversible oxidation process and one irreversible and quai-reversible reduction process. Following the literature,<sup>[4]</sup> anodic potential (E<sup>a</sup>), cathodic potential (E<sup>b</sup>), inflection point (E<sup>(in)</sup>), onset potential (E<sup>onset</sup>) and half-wave potential (E<sup>(1/2)</sup>) of first oxidation wave (E<sub>i</sub>) and second oxidation wave (E<sub>ii</sub>) was calculated.

Potential (V)									
	E <sup>a</sup> <sub>i</sub>	E <sup>a</sup> <sub>ii</sub>	E <sup>c</sup> <sub>i</sub>	E <sup>c</sup> <sub>ii</sub>	E <sup>(in)</sup> <sub>i</sub>	E <sup>(in)</sup> <sub>ii</sub>	E <sup>(1/2)</sup> <sub>i</sub>	E <sup>(1/2)</sup> <sub>ii</sub>	E <sup>onset</sup>
Oxidation	0.89	1.05	-0.81	0.98	0.83	1.06	0.82	1.04	0.77
Reduction	-0.96	-1.32	-	-1.06	-0.83	-1.2	-0.77	-1.17	-0.7

**Table S7:** Summary of electrochemical data. Oxidation and reduction potentials are referenced against ferrocene/ferrocenium (Fc/Fc<sup>+</sup>) couple.

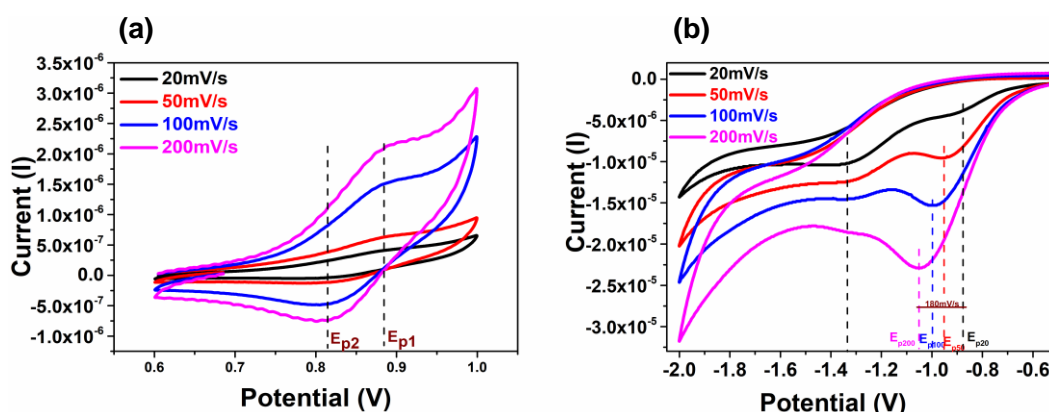


**Figure S6:** (a) First oxidation process and (b) Reduction process recorded at different scan rates. (Concentration of SPS-NR-02 is 100mM)



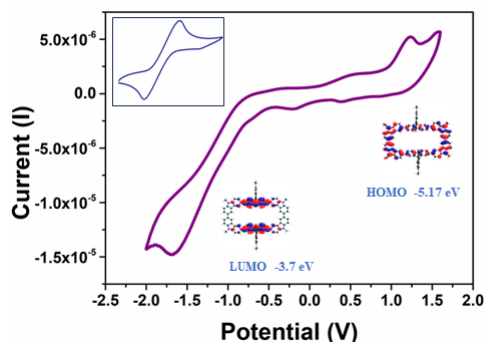


**Figure S7:** Cyclic voltammogram of SPS-NR-02 (100mM) recorded in DCM at 100 mV/s sweep rate and representation of HOMO and LUMO (inset: Cyclic voltammogram of Ferrocene (50mM) recorded in DCM (100mV/s)).

Molecule	HOMO (eV)	LUMO (eV)
Carbazole (donor)	-5.80	-0.63
SFX (acceptor)	-6.10	-0.79
SPS-NR-02	-5.32	-1.05

**Table S8.** Calculated optoelectronic properties of stable conformer SPS-NR-02 at SRSH-LC- $\omega$ HPBE/6-31G(d,p) level of theory using PCM solvent model with DCM.

### 3. Computational Methods and Techniques:

The molecules were optimized to their minimum energy structure at the  $\omega$ B97XD/6-31G(d,p) level of theory. All calculations are performed using the Gaussian16 package.<sup>[5]</sup> The absorption and emission of the first ten excited states were calculated employing the screened range-separated hybrid functional (SRSH) LC- $\omega$ HPBE/6-31G(d,p) method. The calculations were performed in the presence of the PCM solvent model, with toluene as the solvent

#### $\omega$ B97XD/6-31G(d,p):

$\omega$ B97XD is a hybrid density functional that includes long-range dispersion correction. Here X stands for exchange term and D for dispersion. Along with covalent interactions, this functional better describes the dispersion forces, which are important for accurately describing non-covalent interactions.<sup>[6]</sup> In RSH functionals the exchange term is divided in to two components long range and short range with a range separated parameter  $\omega$ .

### **SRSH-LC- $\omega$ HPBE/6-31G(d,p):**

SRSH stands for Screened Range-Separated Hybrid. In SRSH, we use a dielectric constant ( $\epsilon$ ) to regulate the long-range Coulombic interaction.<sup>[7]</sup> This functional is developed to consider the impact of the electrostatic environment on the fundamental gap.

### **NTO analysis:**

Natural transition orbital (NTO) analysis is used to get information about significant orbitals that involved in the electronic transition.<sup>[8]</sup> NTOs for selected excitations are obtained using Multiwfn.

### **Strain Viz analysis:**

Strain visualization programme calculates the total molecular strain along with bond, angle and dihedral angle strain. In this the molecule is first optimized to its lowest energy structure ( $E_{\text{molecule}}$ ) at  $\omega$ B97XD/6-31G(d,p) level of theory. Then molecular fragments are created by removing each portion (monomer unit) from the molecule to release its strain. For example, if a macrocycle has 5 units, we need to create total 5 fragments with 4 units each (only one unit should be removed at a time). Protons were added to the created radical fragments and their single point energy is calculated ( $E_{\text{proton}}$ ). Then each fragment is optimized to minimum energy structure ( $E_{\text{linear}}$ ). The total strain energy is calculated as follows:

$$E_{\text{strain}} = (E_{\text{molecule}} + E_{\text{proton}}) - E_{\text{linear}}$$

### **Counterpoise corrected interaction energy:**

In general, the interaction between two molecules is calculated by the difference between the Energy of the dimer and the energies of individual monomers. But calculating interaction energy with this method, suffers from BSSE (basis set super position error). Here individual basis sets are applied to monomers (A, B) and large basis set (AB) is applied to dimer. Applying individual basis set creates BSSE, in which one monomer takes basis function information from other monomer (basis set and basis functions are used to represent atomic orbitals that construct molecular orbitals). Due to this, when we calculate interaction energy by following formula, the interaction energy is over estimated.

$$E_{\text{int}} = E_{\text{int}}(\text{AB}) - E_{\text{monomer1}}(\text{A}) - E_{\text{monomer2}}(\text{B})$$

In counterpoise corrected method, BSSE is removed by applying large basis set to individual monomers also.<sup>[9]</sup>

$$E_{\text{int}} = E_{\text{int}}(\text{AB}) - E_{\text{monomer1}}(\text{AB}) - E_{\text{monomer2}}(\text{AB})$$

### Strain-viz analysis:

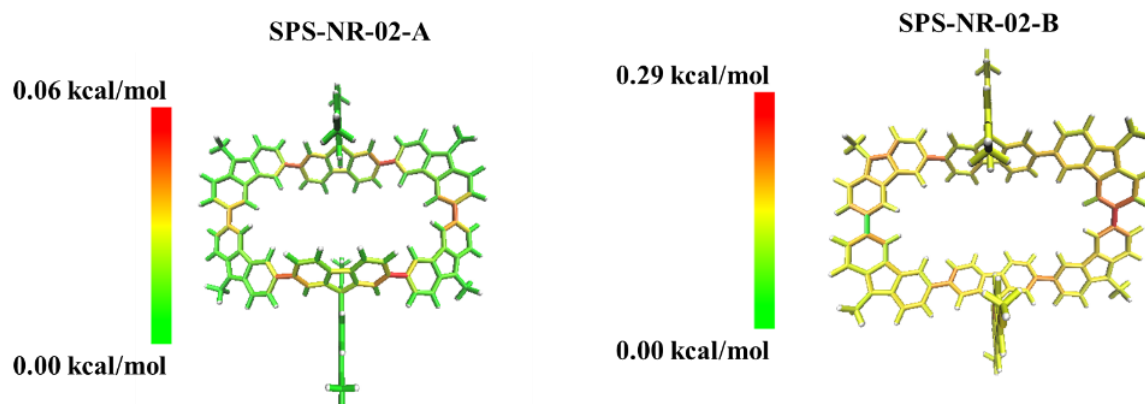


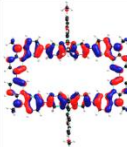
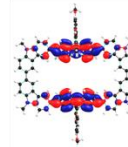
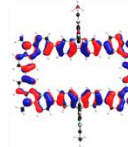
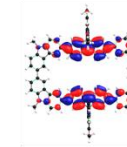
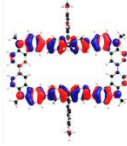
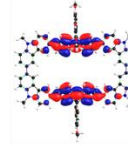
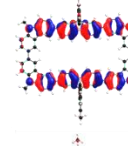
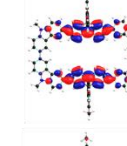
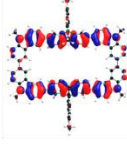
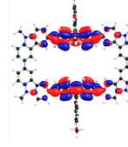
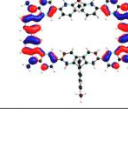
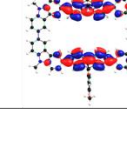
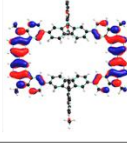
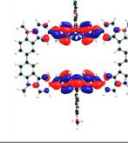
**Figure S8:** Pictorial representation of Strain analysis of SPS-NR-02 obtained at  $\omega$ B97XD/6-31G(d,p) level of theory.

Compound	Bond strain	Angle strain	Dihedral angle strain	Total strain
SPS-NR-02-A	0.06	0.44	1.45	2.05
SPS-NR-02-B	1.22	0.00	4.45	5.67

**Table S9:** Strain analysis of SPS-NR-02 obtained at  $\omega$ B97XD/6-31G(d,p) level of theory. Energies are given in kcal/mol.

### Natural Population Analysis:

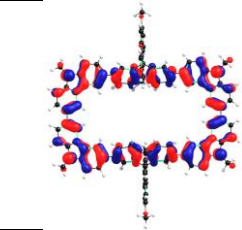
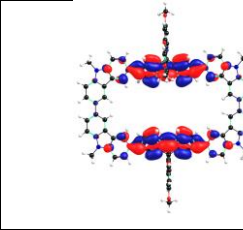
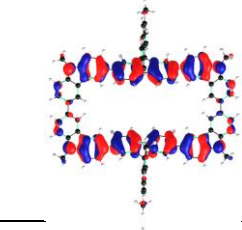
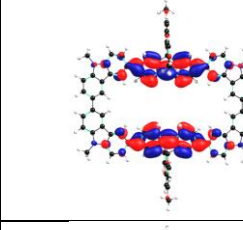
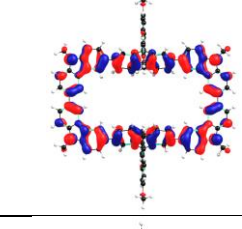
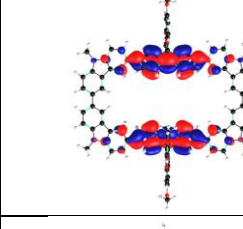
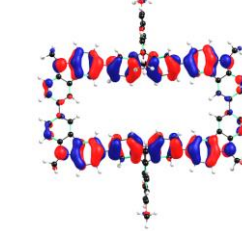
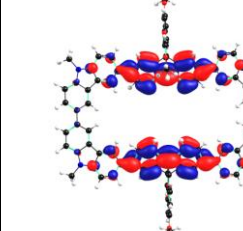
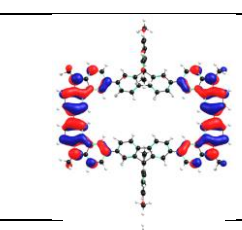
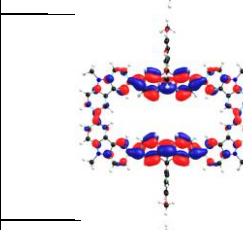
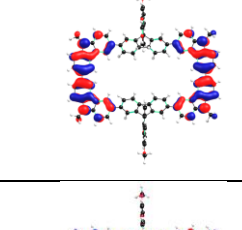
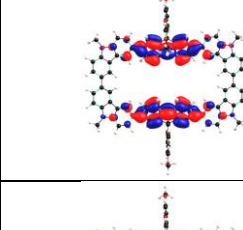
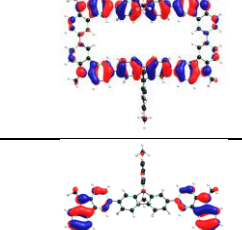
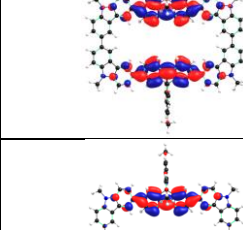
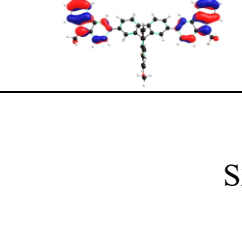
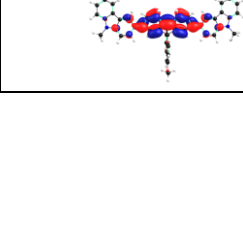
The nature of excited states was analyzed through Natural Transition Orbital (NTO) analysis using the Multiwfn program.

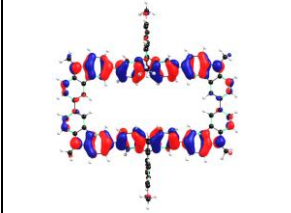
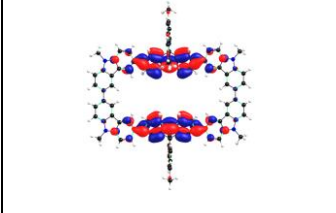
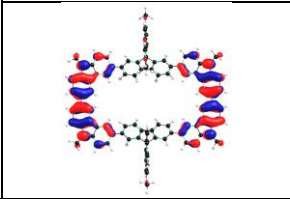
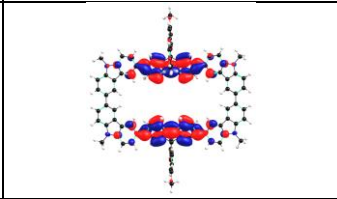
Absorption	Hole	electron	weightage	Emission	Hole	electron	weightage
$S_0 \rightarrow S_2$ $\lambda_{\text{abs}} = 336 \text{ nm}$ $f = 2.76$			66%	$S_2 \rightarrow S_0$ $\lambda_{\text{ems}} = 380 \text{ nm}$ $f = 3.58$			61%
			29%				34%
			52%				86%
$S_0 \rightarrow S_{10}$ $\lambda_{\text{abs}} = 306 \text{ nm}$ $f = 0.43$			41%				

**Figure S9.** NTOs for the absorption bands (left) and emission bands (right) obtained at SRSH-LC- $\omega$ HPBE/6-31G(d,p) level of theory using toluene as solvent.

SPS-NR-02	Dipole moment ( $\mu$ ) (debye)	Natural Population Analysis		Amount of charge transferred $ e $
		Sum of Charges on all donor units (carbazole)	Sum of Charges on all acceptor units (SFX unit)	
Ground state	0.544	0.08	-0.08	0.08
Excited State-1	0.622	0.34	-0.34	0.34
Excited State-2	0.554	0.36	-0.36	0.36
Excited State-3	0.329	0.04	-0.04	0.04
Excited State-4	1.474	0.04	-0.04	0.04
Excited State-5	0.154	0.05	-0.05	0.05
Excited State-6	1.010	0.04	-0.04	0.04
Excited State-7	0.573	0.50	-0.50	0.50
Excited State-8	1.008	0.59	-0.59	0.59
Excited State-9	0.796	0.36	-0.36	0.36
Excited State-10	0.791	0.41	-0.41	0.41

**Table S10:** Ground and excited state dipole moments of SPS-NR-02 calculated at SRSH-LC- $\omega$ HPBE/6-31G(d,p) level of theory using DCM as solvent with PCM solvent model.

SPS-NR-02	Hole	electron	weightage
Excited state-1			68
			23
Excited state-2			64
			31
Excited state-7			83
Excited state-8			85
Excited state-9			50
			38

Excited state-10			49
			45

**Table S11:** NTO analysis of SPS-NR-02 for some of the excited states performed at SRSH-LC- $\omega$ HPBE/6-31G(d,p) level of theory using DCM as solvent with PCM solvent model.

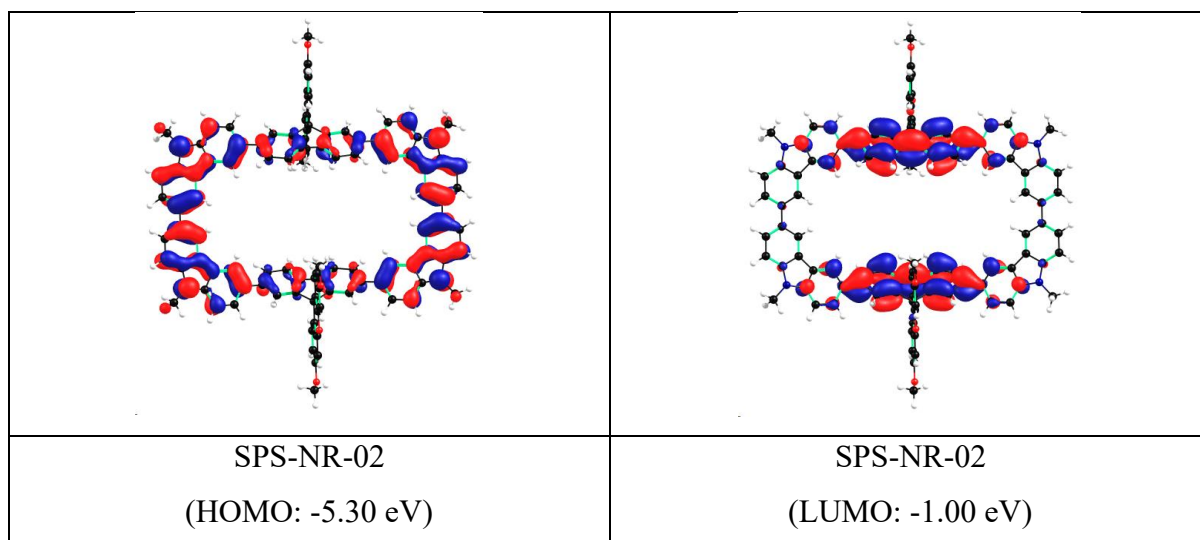


**Figure S10:** HOMO and LUMO wavefunction distribution in SPS-NR-02 macrocycle as determined at SRSH-LC- $\omega$ HPBE/6-31G(d,p) level of theory.

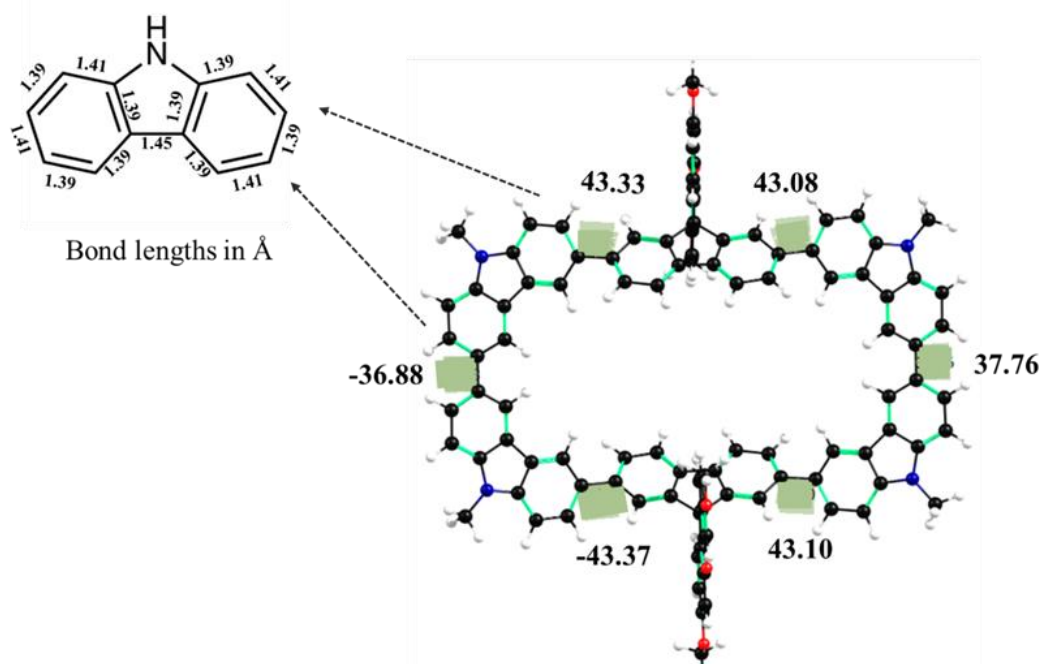


**Figure S11:** Geometrical parameters of SPS-NR-02 obtained at  $\omega$ B97XD/6-31G(d,p) level of theory.

#### 4. Host-Guest analysis:

To the solution of SPS-NR-02 (concentration was  $2 \times 10^{-5}$  M) in toluene was added the solutions of  $C_{60}$  (concentrations ranging from  $8 \times 10^{-6}$  M to  $10^{-4}$  M) in toluene at  $25^\circ\text{C}$ . Fluorescence spectroscopy of SPS-NR-02 at different host-guest concentrations was recorded (Figure S10). Concentration of  $C_{60}$  was plotted against the ratio of initial fluorescence intensity ( $I_0$ ) to fluorescence intensity ( $I$ ) after addition of  $C_{60}$  to get the Stern-Völmer plot. The binding constant ( $K_a$ ) was determined using the equation

$$\frac{I_0}{I} = \frac{(1 + AK_a[G])}{(1 + K_a[G])}$$

Where  $I_0$  denotes the initial fluorescence intensity,  $I$  denote the fluorescence intensity after addition of  $C_{60}$ ,  $[G]$  is the concentration of guest and  $A$  is the ratio of proportionality constants. For dynamic quenching, the equation deduces to

$$\frac{I_0}{I} = (1 + K_a[G])$$

The binding association calculation from the slope of the linear plot (Figure S10) was  $K_{sv} = K_a = 9.95 \times 10^4 \text{ M}^{-1}$ , Pearson's  $r$  was 0.98413 and correlation coefficient  $R^2$  was 0.96402.



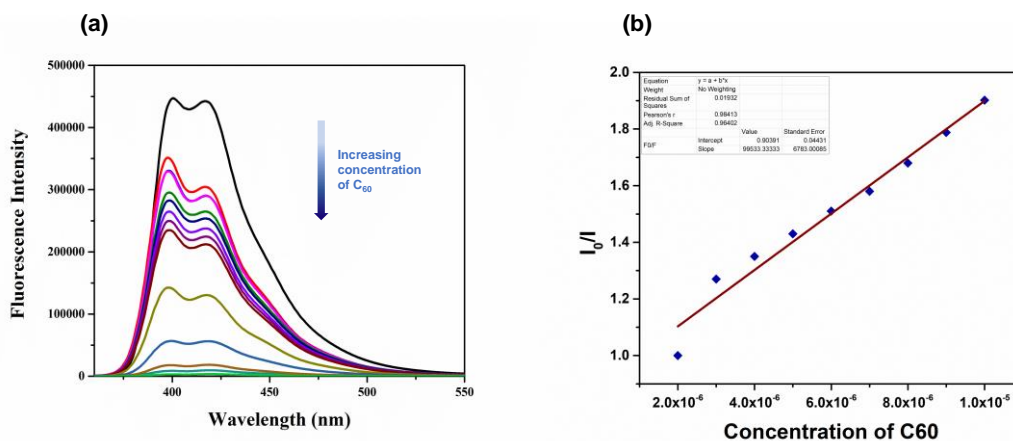


**Figure S12:** (a) Fluorescence quenching of SPS-NR-02 upon addition of C<sub>60</sub> in toluene. (b) Stern-Völmer fitting for the binding of C<sub>60</sub> to SPS-NR-02 in toluene.

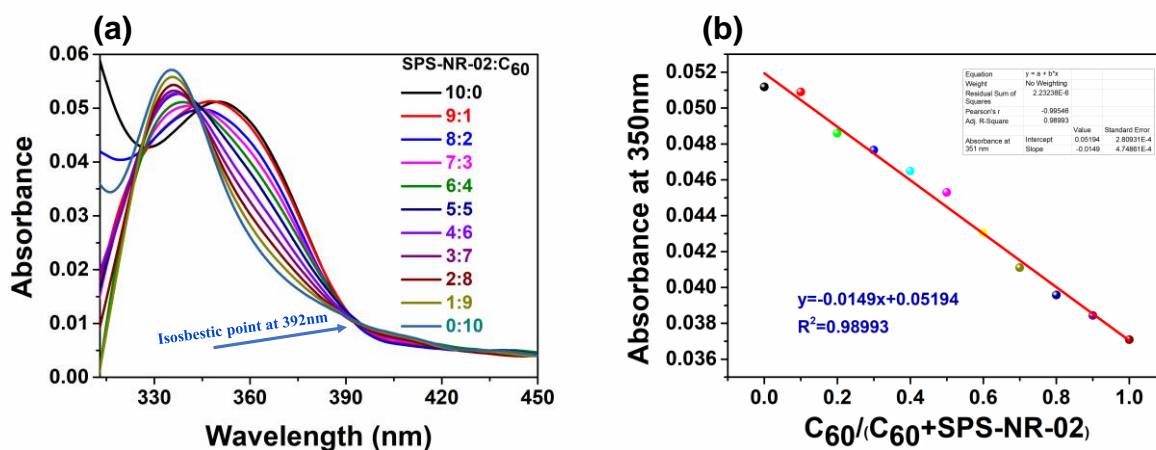


**Figure S13:** (a) UV-vis absorption spectra of different ratios of SPS-NR-02 ( $5 \times 10^{-6}$ M) and C<sub>60</sub> ( $5 \times 10^{-6}$ M) in O-DCB at room temperature. (b) Linear plot of change in absorbance at 351nm against mole fraction of C<sub>60</sub>.

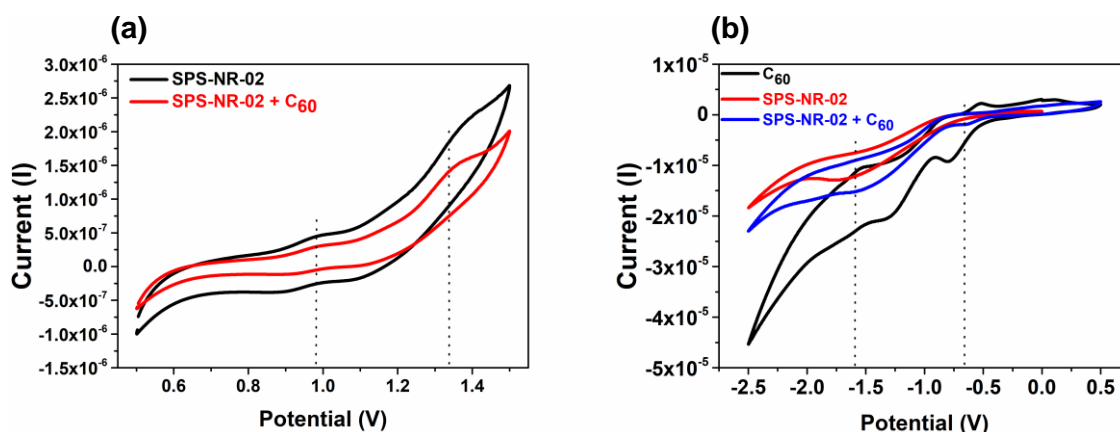


**Figure S14:** (a) Oxidation and (b) Reduction process of SPS-NR-02 when equimolar amounts of  $C_{60}$  was added. (Concentration of SPS-NR-02 and  $C_{60}$  is 100mM and scan rate is 100mv/s).

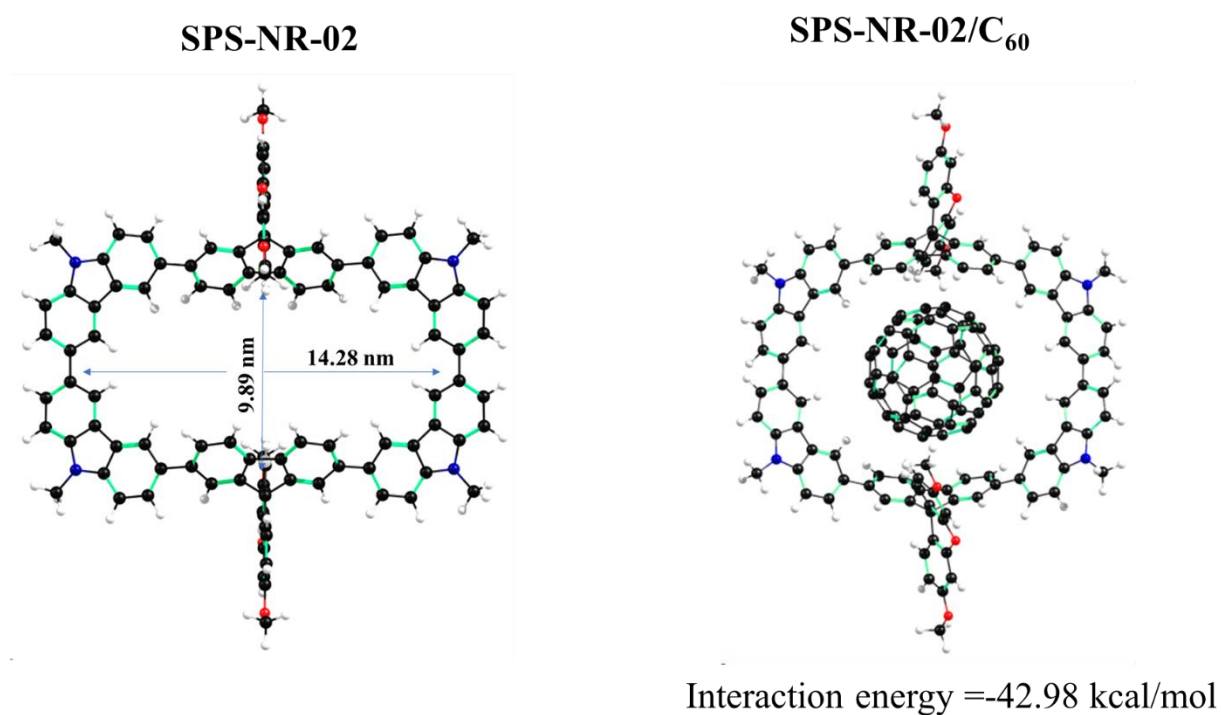


**Figure S15:** Optimized geometries of SPS-NR-02 and SPS-NR-02/ $C_{60}$  obtained at  $\omega$ B97XD/6-31G(d,p) level of theory.

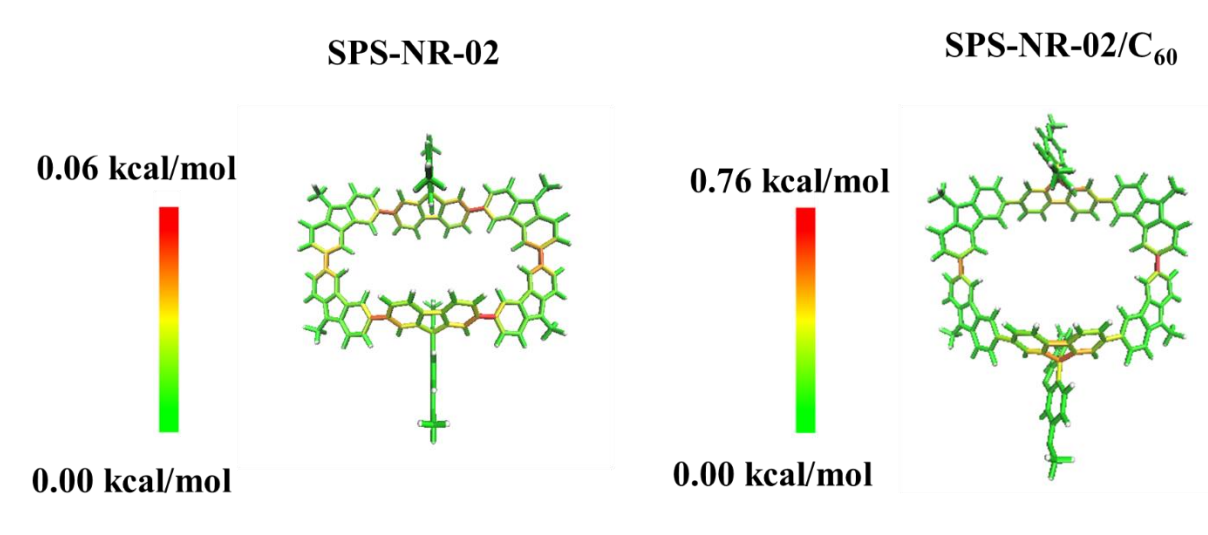


**Figure S16:** Strain energies of SPS-NR-02 and SPS-NR-02/C<sub>60</sub> obtained at  $\omega$ B97XD/6-31G(d,p) level of theory.

Compound	Bond strain	Angle strain	Dihedral angle strain	Total strain
SPS-NR-02	0.06	0.44	1.45	2.05
SPS-NR-02/C <sub>60</sub>	0.73	2.79	15.29	18.80

**Table S12:** Strain analysis of SPS-NR-02 and SPS-NR-02/C<sub>60</sub> obtained at  $\omega$ B97XD/6-31G(d,p) level of theory. Energies are given in kcal/mol.

Energy components	Energy in kcal/mol
Electrostatic	-39.75
Exchange	76.25
Induction	-13.04
Dispersion	-105.75
<b>Total interaction</b>	<b>-82.29</b>

**Table S13:** Calculated various interaction energy components as determined using SAPT/cc-pvdz for macrocycle-C<sub>60</sub> complex.

## Space-charged limited current measurements:

### Device Fabrication:

FTO substrates ( $15 \Omega/\square$ , from Greatcell Solar Materials, Australia) substrates were first patterned using 2M HCl solution and Zinc powder. Subsequently, patterned FTO substrates were sequentially cleaned using a 3% soap solution (HelmanexIII, Sigma Aldrich), followed by deionized water, acetone, and isopropyl alcohol in an ultrasonicator (BioBee, Bangalore, India) for 20 minutes each. Cleaned substrates were then dried under the gentle flow of ultra-pure nitrogen gas. The FTO substrates were then exposed to UV Ozone cleaner (BioBee, Bangalore, India) for 20 minutes at 50 °C.

Hole only devices were fabricated in FTO/PEDOT: PSS (~25 nm)/SPS-NR-02(~100 nm)/MoO<sub>3</sub>(~ 10 nm)/Ag (~ 100 nm) architecture whereas electron only devices were fabricated in FTO/ZnO (30 nm)/ SPS-NR-02(~ 100 nm)/BCP (~2-5 nm)/Al (100 nm). The PEDOT: PSS and ZnO were used as hole transporting and electron transporting material in hole only and electron only devices because they were found suitable with the HOMO and LUMO of SPS-NR-02 to establish ohmic contact. For hole only devices, 100  $\mu$ l of PEDOT: PSS was spin coated statically at 4500 rpm for 65 seconds on UV Ozone treated FTO substrates. The spin-coated substrates were then annealed at 150°C for 20 minutes under ambient conditions. Subsequently, SPS-NR-02 solution in chloroform (10 mg/ml) was spin-coated onto PEDOT: PSS coated substrate at 1500 rpm for 45 seconds to obtain 100 nm thick films. The samples were then placed under thermal evaporator (Hind High Vacuum, India) to deposit 10 nm of MoO<sub>3</sub> and 100 nm of Ag sequentially at  $3 \times 10^{-6}$  mbar base pressure to complete the hole only devices.

To extract holes and electrons mobilities of material, hole, and electron only devices are being fabricated. In SCLC technique material is sandwiched between two electrodes among which one electrode should serve as infinite reservoir of charges (i.e. an ohmic contact with HOMO for hole only devices and with LUMO for electron only devices) a condition necessary to achieve SCLC regime.[31] The complete fabrication and characterization details are provided in ESI (Table S14). Typically, charge carrier mobility in organic materials (in thin films) is field dependent and can be extracted using modified Mott-Gurney equation

$$J = \frac{9}{8} \mu \epsilon_r \epsilon_o \frac{V^2}{d^3} \exp \left( 0.891 \gamma \sqrt{\frac{V}{d}} \right) \quad (2)$$

where  $J$  represents the measured current density,  $\epsilon_0$  denotes the permittivity of free space,  $\epsilon_r$  represents the relative dielectric constant of the material (3.8),  $V$  stands for the applied voltage,  $d$  indicates the thickness of the active layer of the material,  $\mu$  signifies the mobility, and  $\gamma$  represents the fitting parameter that characterizes the strength of the electric field dependence of mobility.

For fabricating electron only devices firstly the ZnO sol-gel solution was prepared by vigorously stirring 200 mg of Zinc Acetate Dihydrate in 52 mg of ethanolamine and 2 ml of 2-Methoxyethanol overnight at room temperature. Subsequently, the ZnO sol-gel solution was spin-coated onto previously cleaned and UV ozone treated FTO substrates at 4500 rpm for 65 seconds. The spin-coated substrates were then annealed at 180°C for 1 hour under ambient conditions. **SPS-NR-02** solution in chloroform (10 mg/ml) was then spin-coated at 1500 rpm for 45 seconds to obtain 100 nm thick film followed by dynamic spin coating of BCP solution (0.5 mg/ml in anhydrous IPA). The devices were then completed by evaporating 100 nm of aluminium under  $3 \times 10^{-6}$  mbar base pressure. The samples for both hole only and electron only devices have an active area of 6.6 mm<sup>2</sup> calculated using the overlap area of both electrodes. All the devices were fabricated inside a glove box (GS Germany, O<sub>2</sub> < 100 PPM, H<sub>2</sub> < 0.2 PPM).

Current- voltage characteristics were carried out using Keithley 2450 source meter (Tektronix, USA). The thickness measurement of different layers was performed using Dektak Surface profile while dielectric constant of **SPS-NR-02** was measured using high-frequency LCR meter ZM2376 (NF corporation Japan) with an applied oscillation level voltage of 1V over the frequency range 20Hz-2MHz.”

Sample No.	Hole Mobility (cm <sup>2</sup> V <sup>-1</sup> s <sup>-1</sup> ) (x 10 <sup>-3</sup> )	Electron Mobility (cm <sup>2</sup> V <sup>-1</sup> s <sup>-1</sup> ) (x 10 <sup>-3</sup> )
1	4.92	1.84
2	5.17	1.96
3	3.97	2.15
4	4.43	2.00
5	5.24	1.40
<b>Average</b>	4.75	1.87
<b>STDEV</b>	0.54	0.29

**Table S14:** Statistics of 5 best devices of both hole and electron mobility.

## 5. NMR Spectra:

### 5.1 $^1\text{H}$ and $^{13}\text{C}$ NMR of SFX:

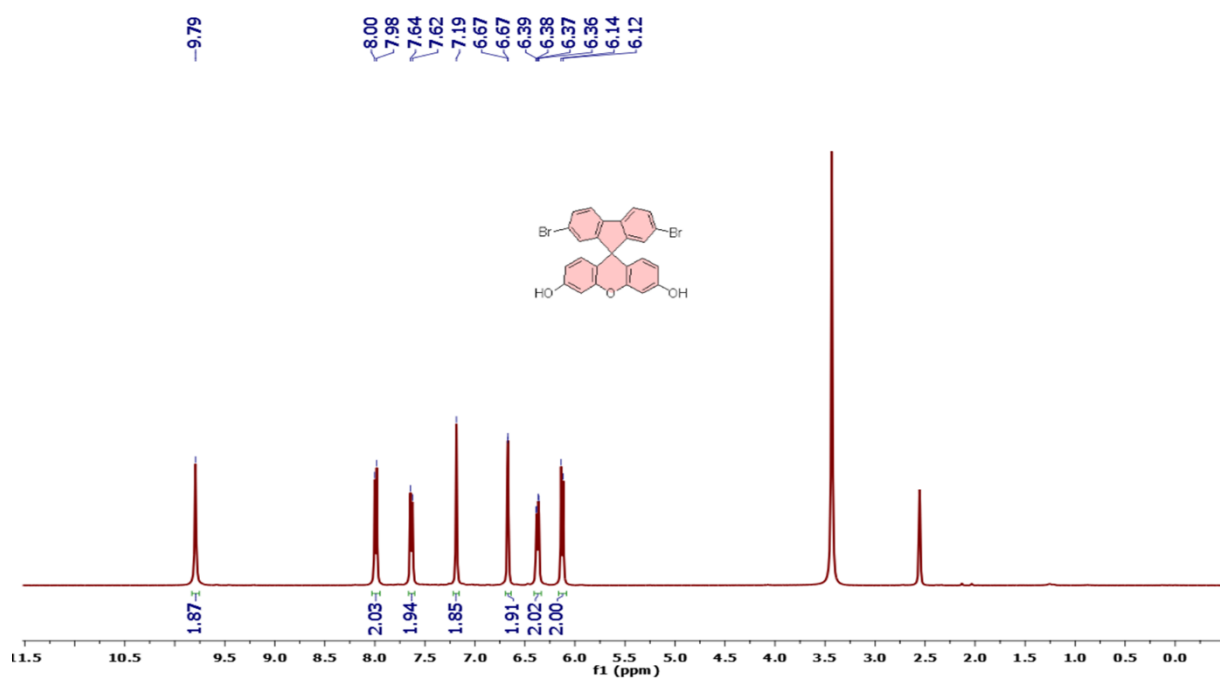


Figure S17:  $^1\text{H}$  NMR of SFX, 400MHz, DMSO- $d_6$

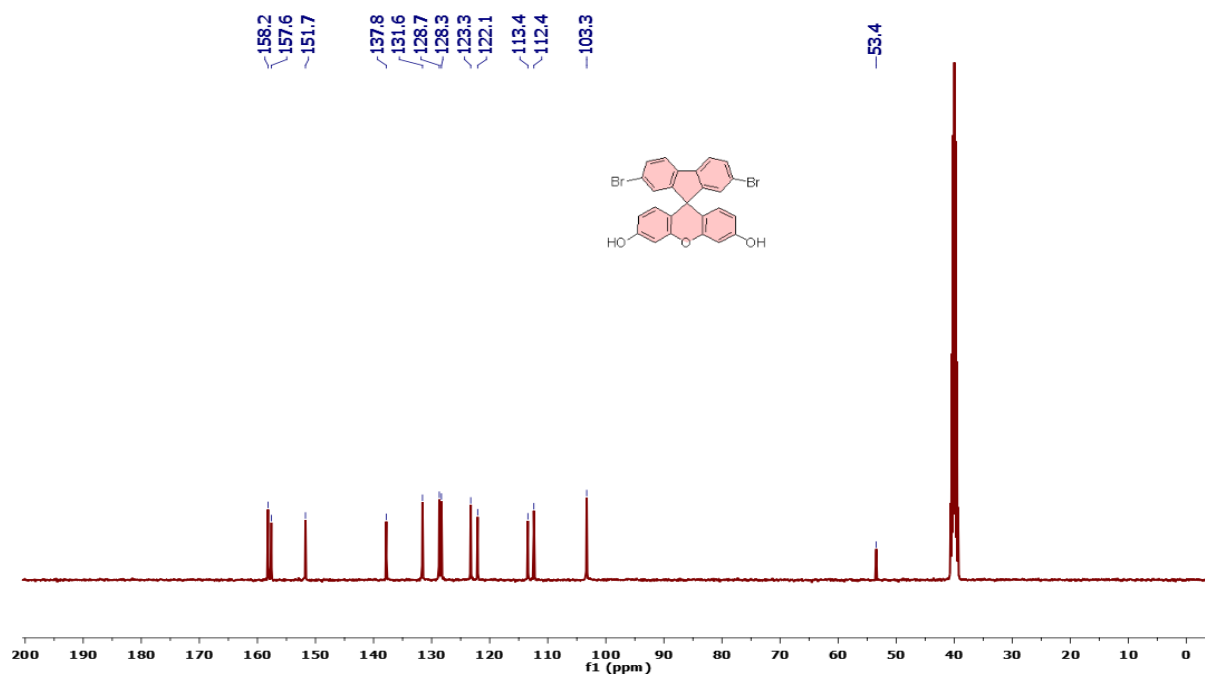


Figure S18:  $^{13}\text{C}$  NMR of SFX, 101MHz, DMSO- $d_6$

## 5.1 $^1\text{H}$ and $^{13}\text{C}$ NMR of SFX-OR:

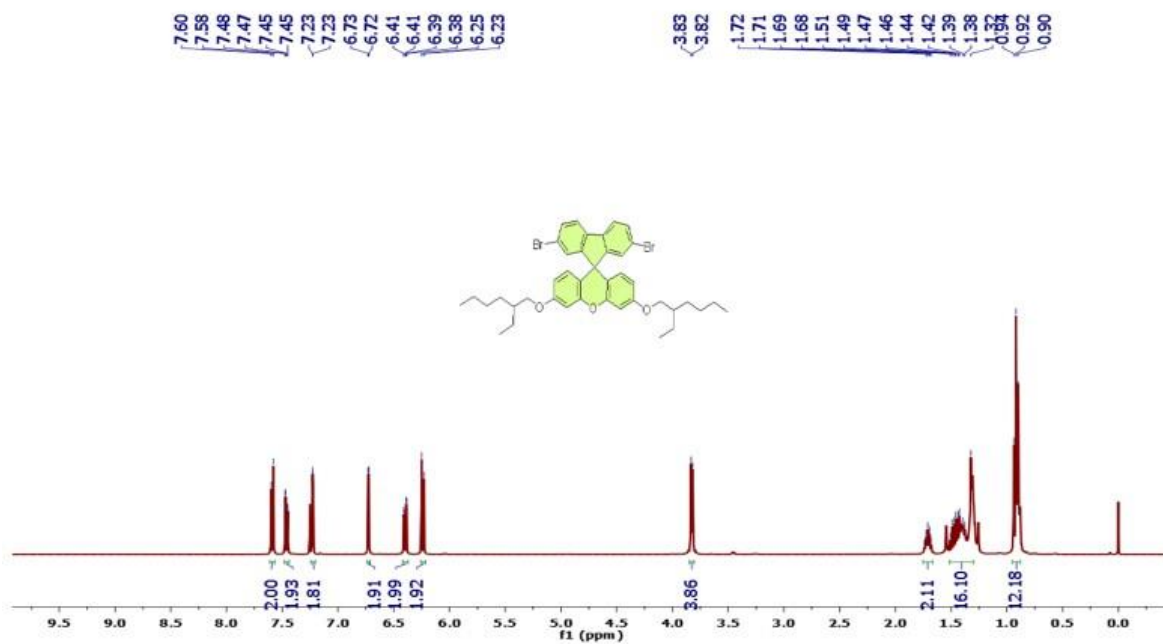


Figure S19:  $^1\text{H}$  NMR of SFX-OR, 400MHz,  $\text{CDCl}_3$ .

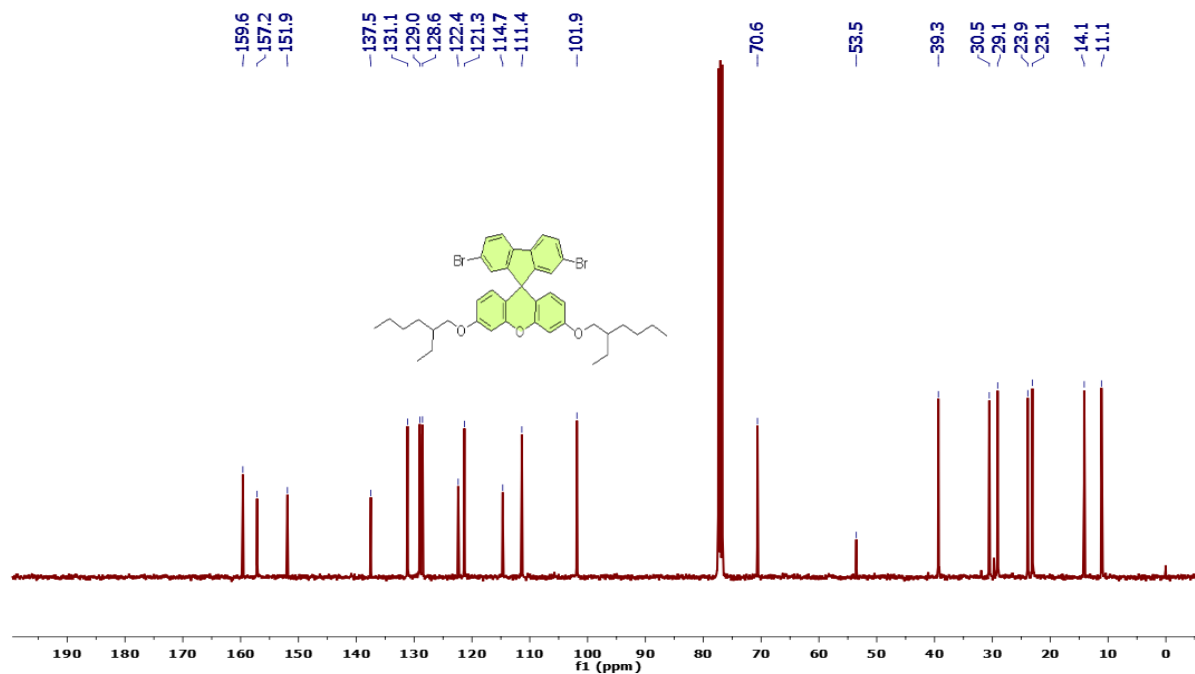


Figure S20:  $^{13}\text{C}$  NMR of SFX-OR, 101MHz,  $\text{CDCl}_3$ .

## 5.2 $^1\text{H}$ and $^{13}\text{C}$ NMR of Bpin-SFX:

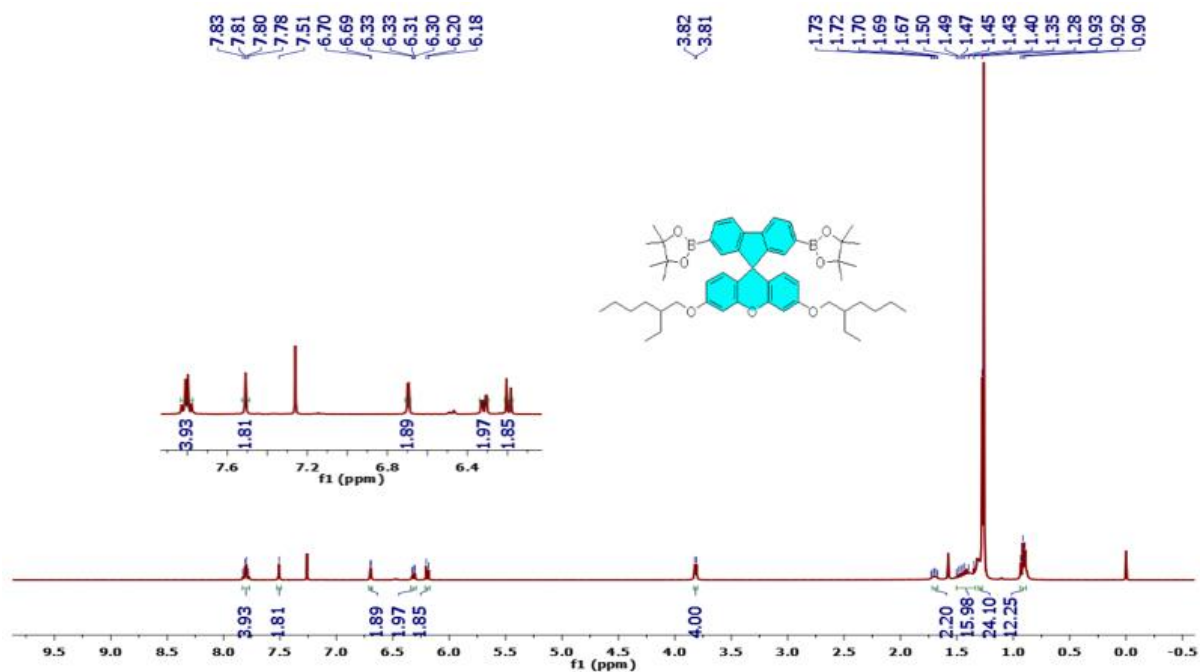


Figure S21:  $^1\text{H}$  NMR of Bpin-SFX, 400MHz,  $\text{CDCl}_3$ .

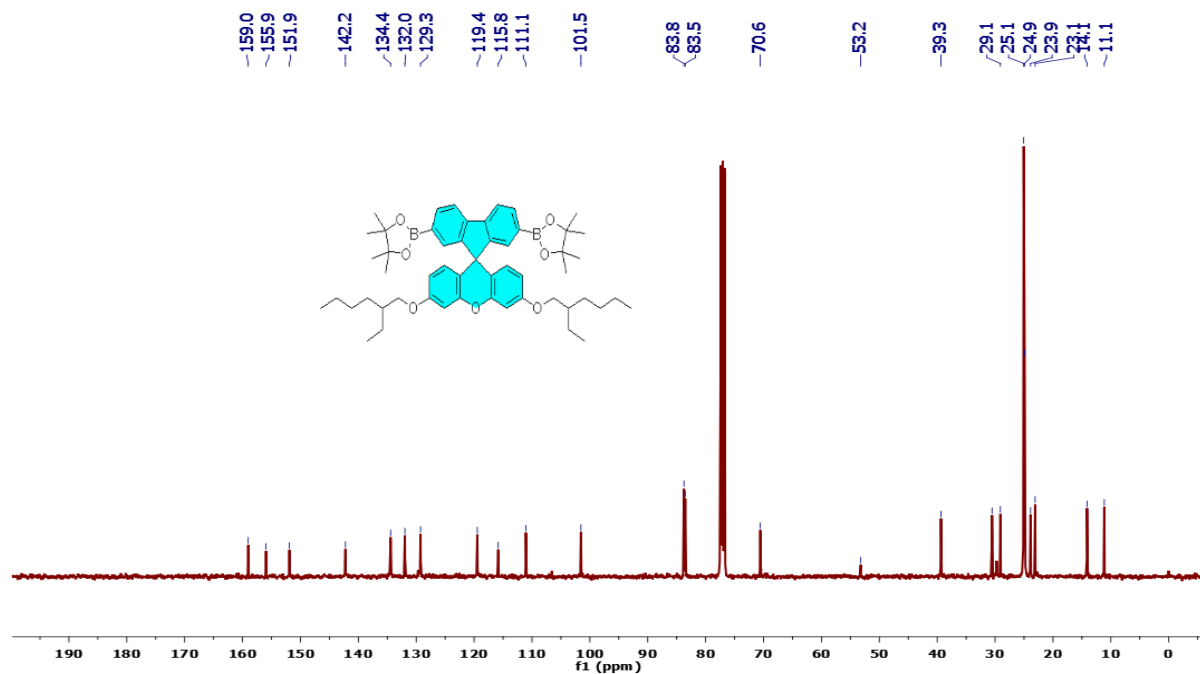


Figure S22:  $^{13}\text{C}$  NMR of Bpin-SFX, 101MHz,  $\text{CDCl}_3$ .



### 5.3 $^1\text{H}$ and $^{13}\text{C}$ NMR of CSC:

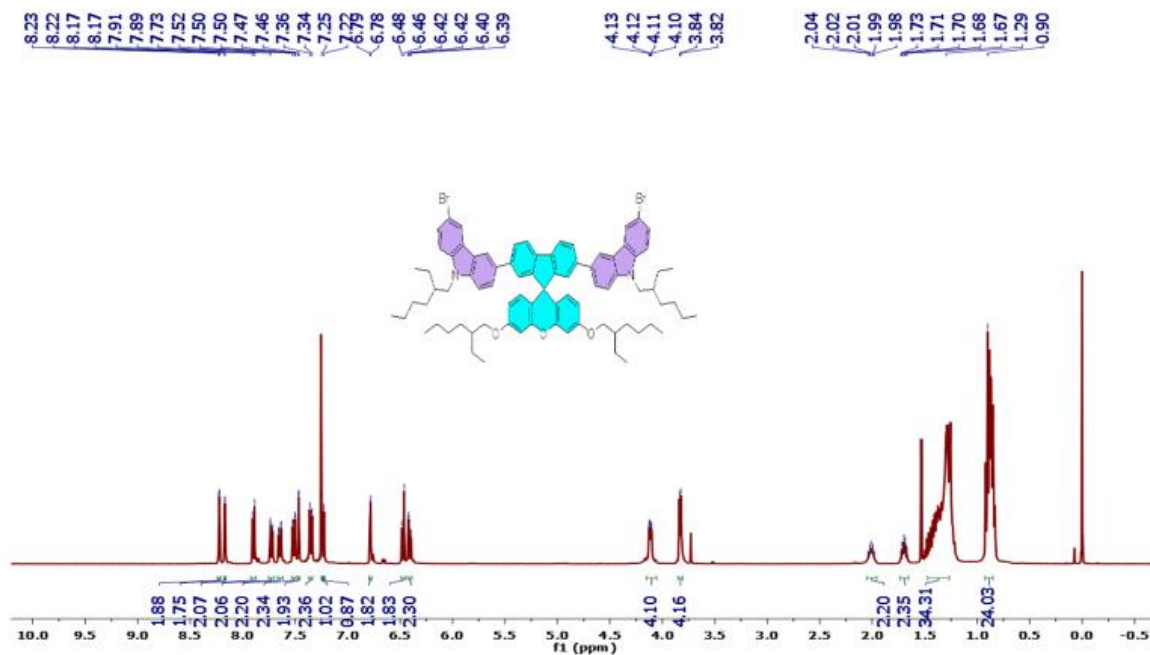


Figure S23:  $^1\text{H}$  NMR of CSC, 400MHz,  $\text{CDCl}_3$ .

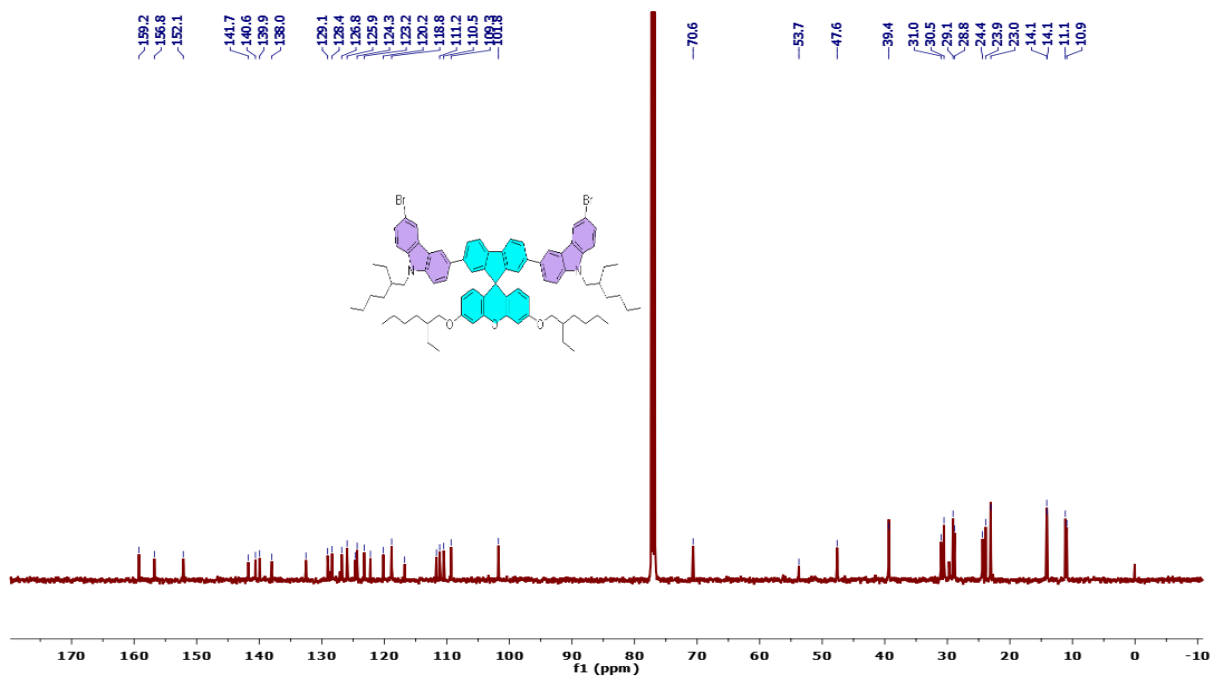


Figure S24:  $^{13}\text{C}$  NMR of CSC, 126MHz,  $\text{CDCl}_3$ .

## 5.4 $^1\text{H}$ and $^{13}\text{C}$ NMR of Bpin-CSC:

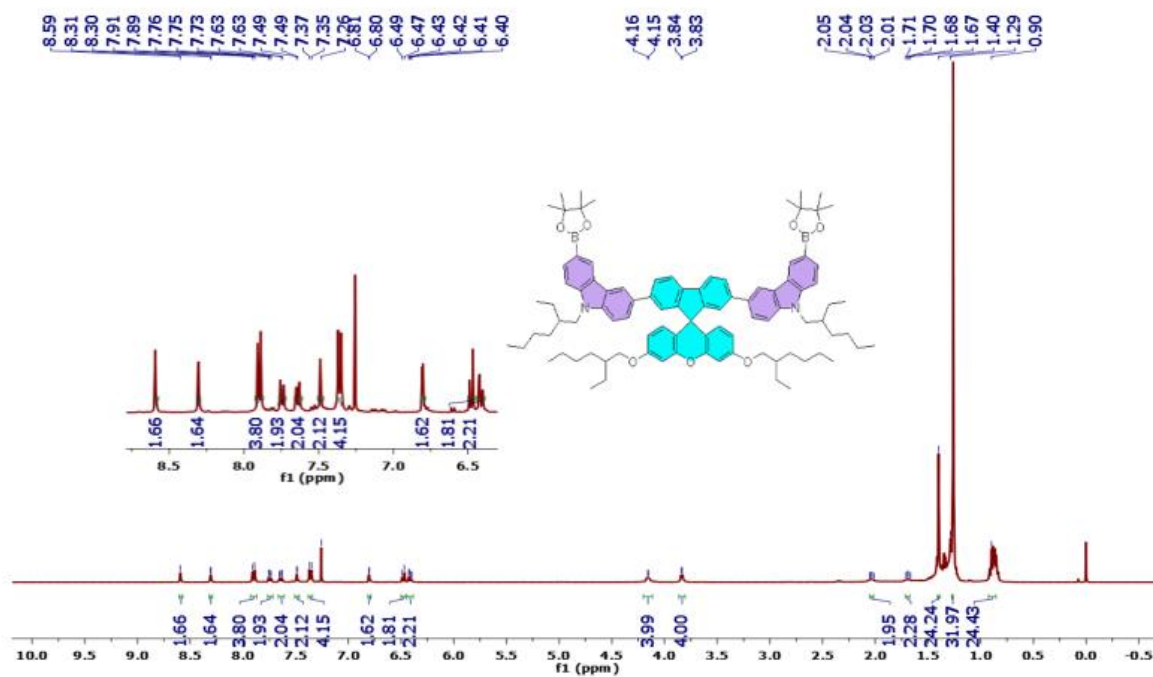


Figure S25:  $^1\text{H}$  NMR of Bpin-CSC, 400MHz,  $\text{CDCl}_3$ .

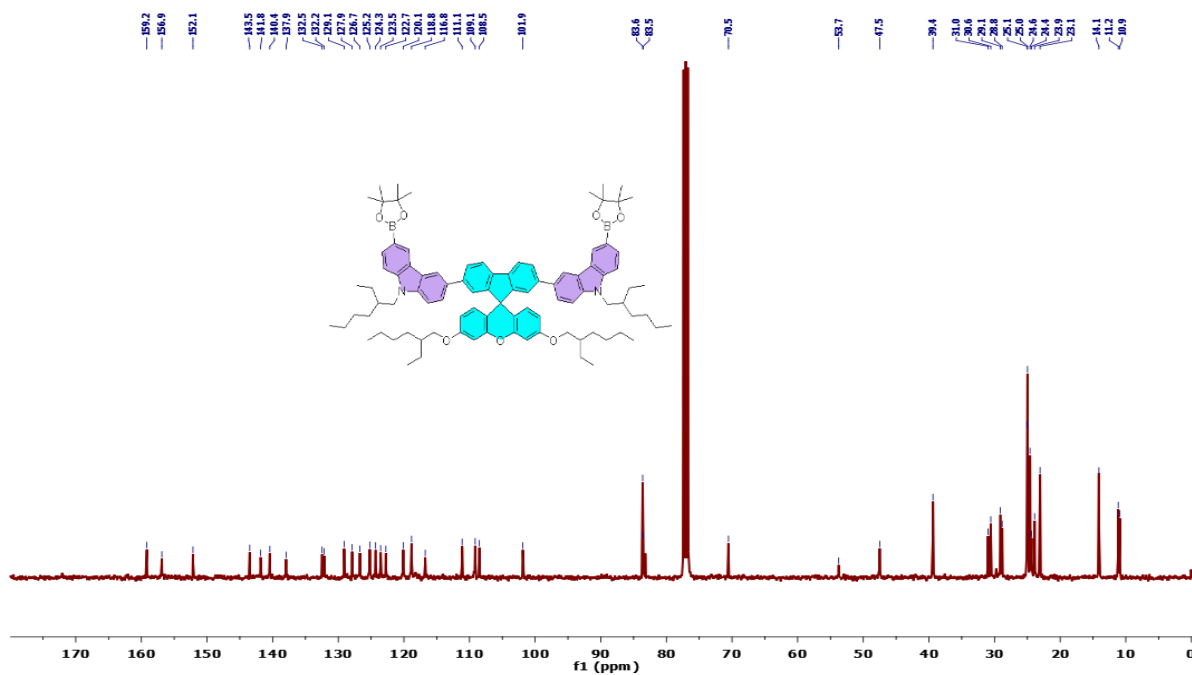


Figure S26:  $^{13}\text{C}$  NMR of Bpin-CSC, 101MHz,  $\text{CDCl}_3$ .

5.5  $^1\text{H}$  and  $^{13}\text{C}$  NMR of SPS-NR-02:

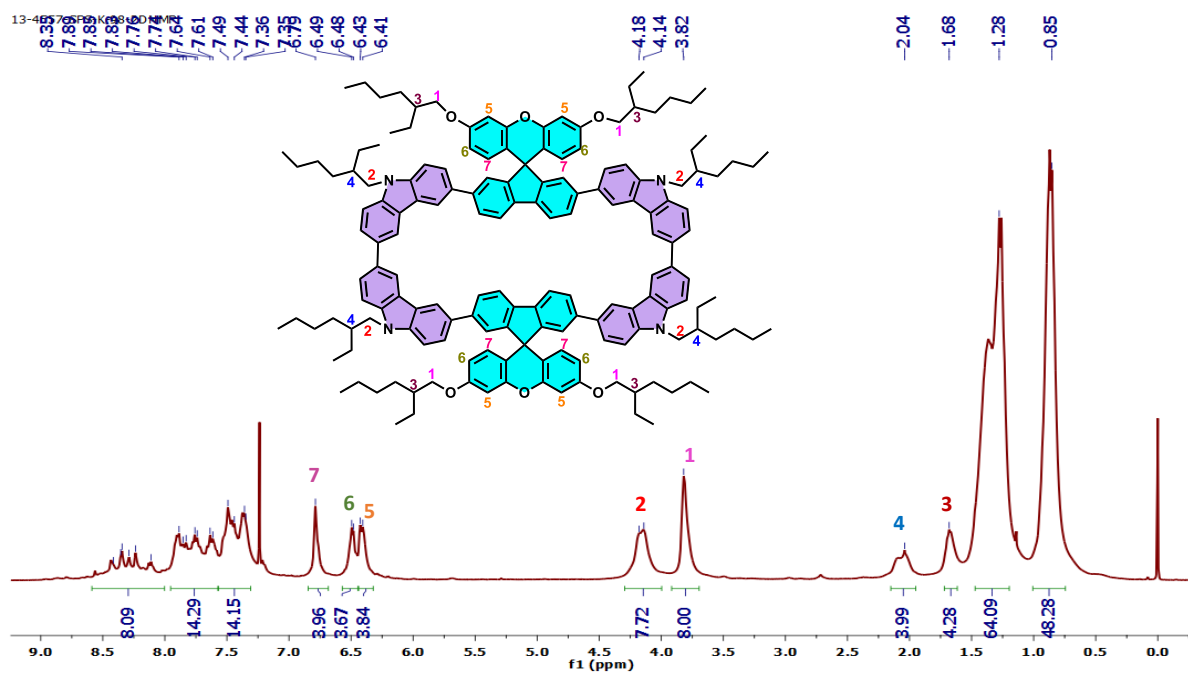


Figure S27:  $^1\text{H}$  NMR of SPS-NR-02, 400MHz,  $\text{CDCl}_3$ .

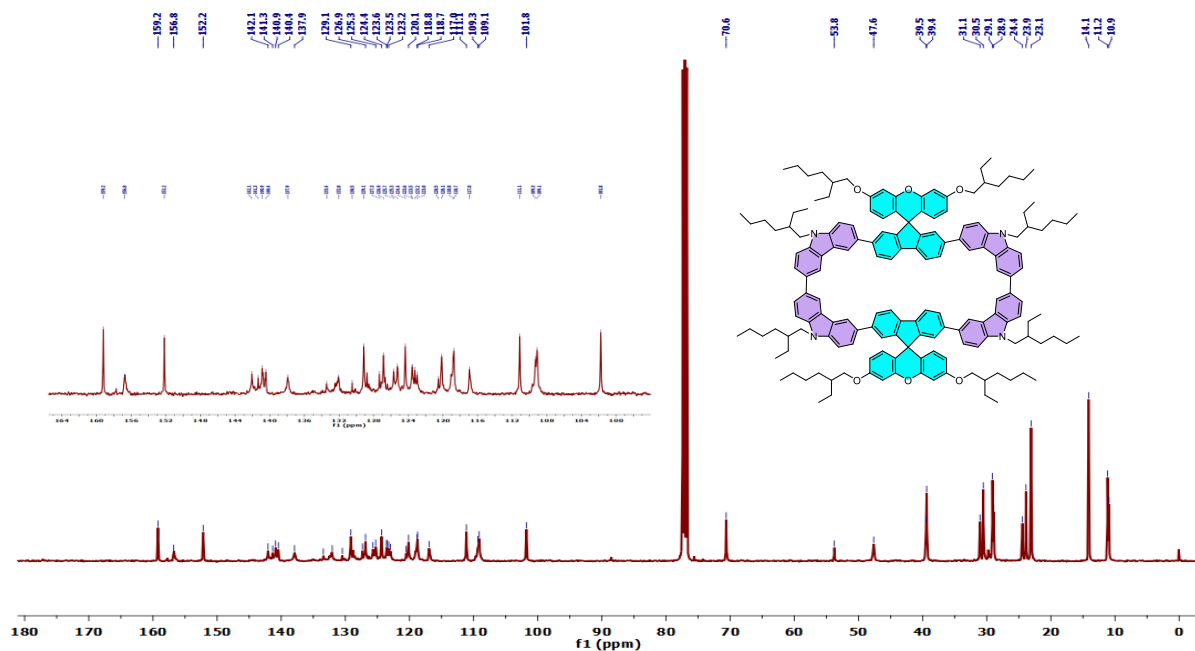
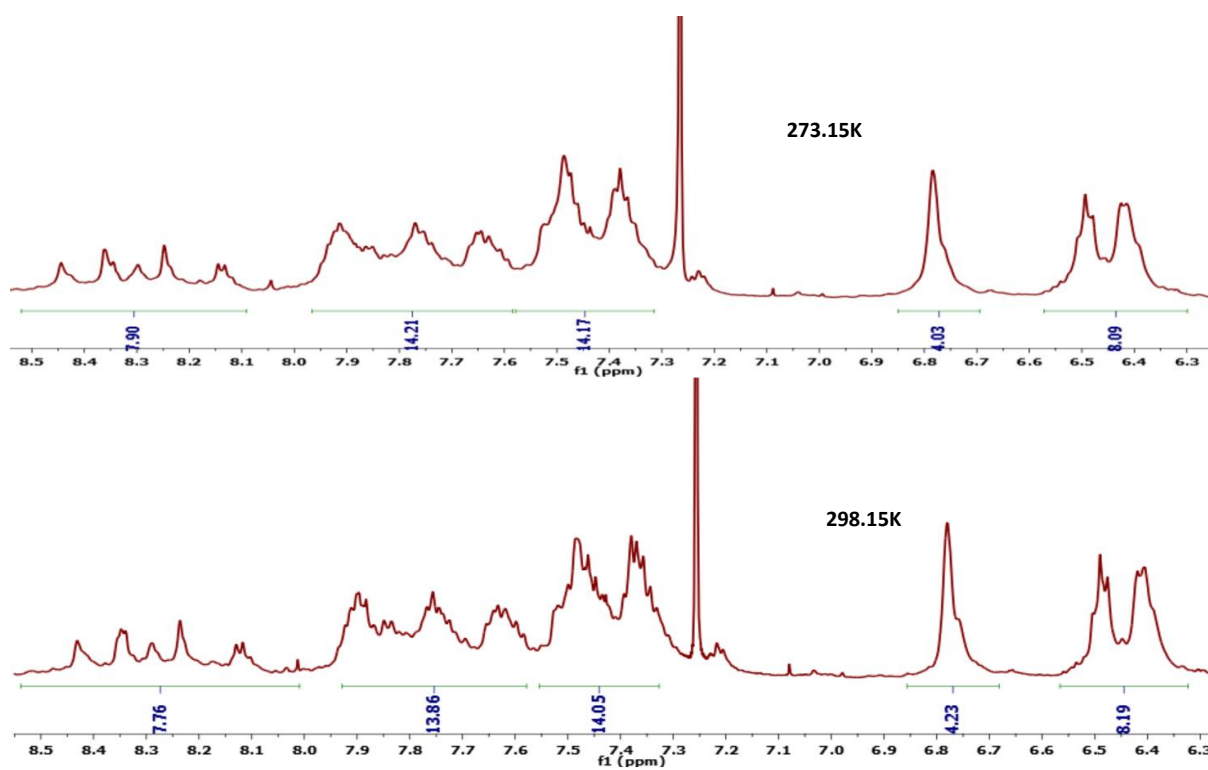
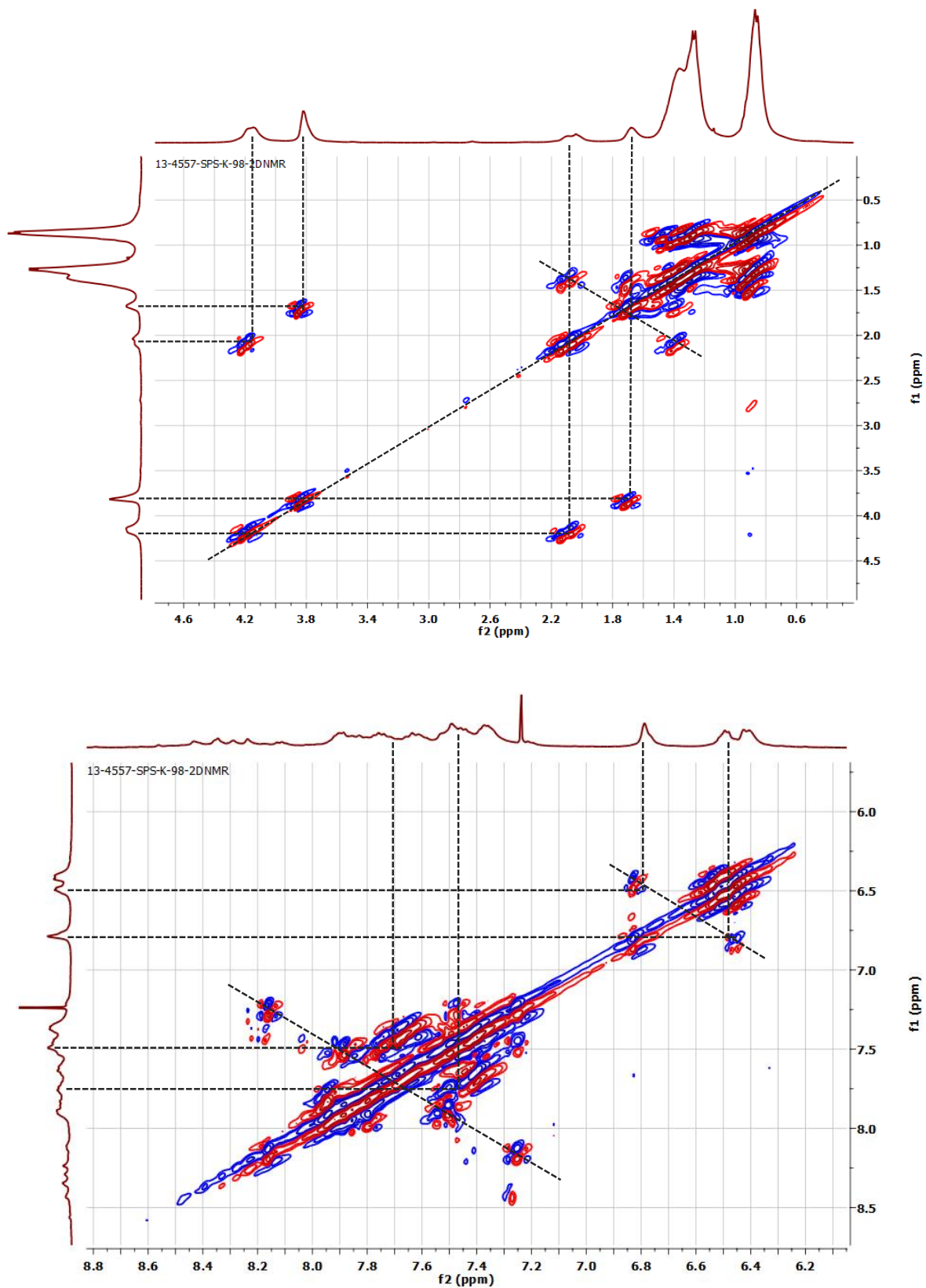


Figure S28:  $^{13}\text{C}$  NMR of SPS-NR-02, 101MHz,  $\text{CDCl}_3$ .



**Figure S29:**  $^1\text{H}$  NMR of SPS-NR-02 recorded at 25°C (bottom) and at 0°C (top), 600 MHz,  $\text{CDCl}_3$ .



**Figure S30:** Expanded 2D  $^1\text{H}$ - $^1\text{H}$  COSY NMR spectrum of SPS-NR-02, 400MHz,  $\text{CDCl}_3$ . Aliphatic region (top), aromatic region (bottom)

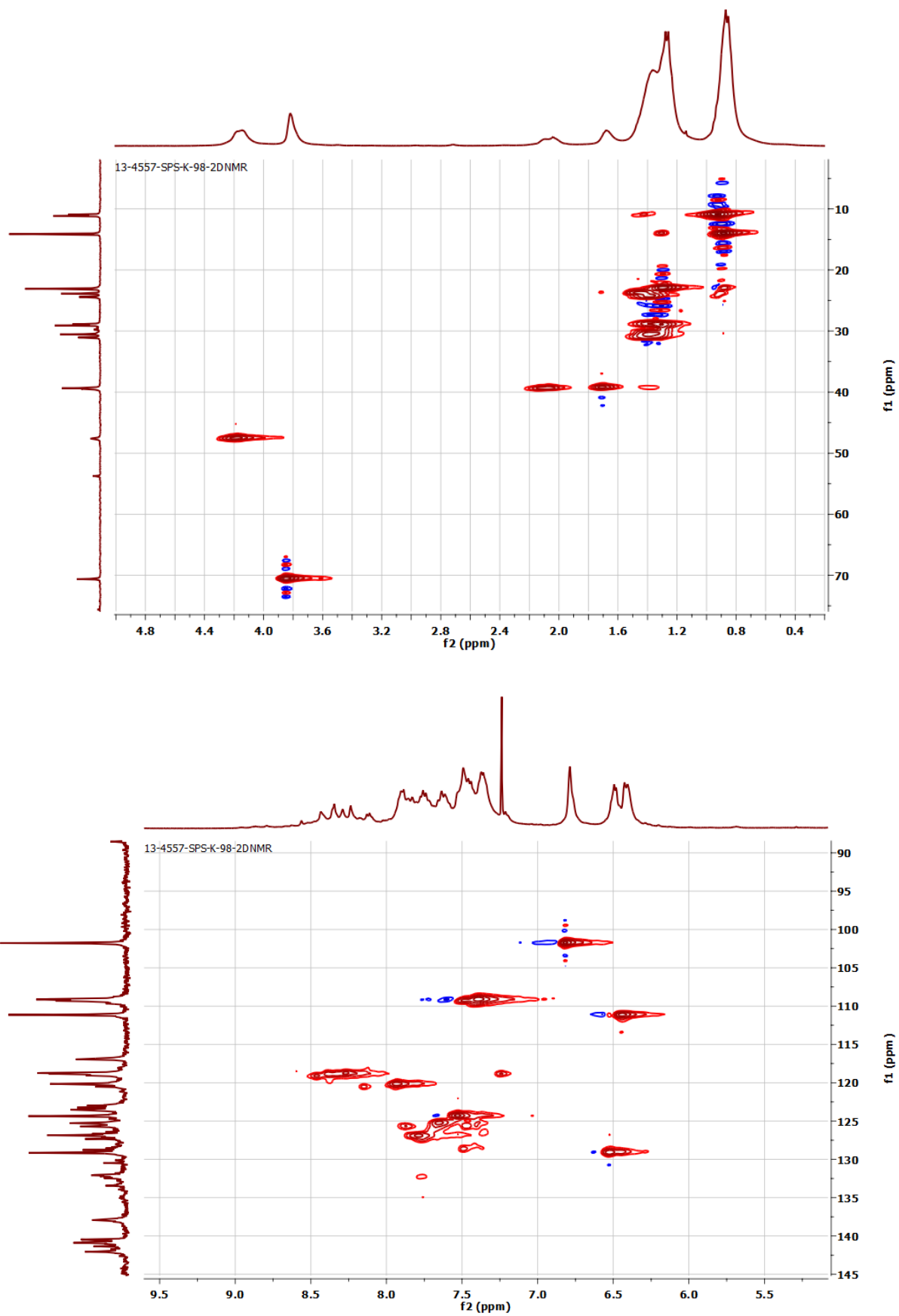


**Figure S31:** Expanded 2D (H,C)-HSQC NMR spectrum of SPS-NR-02, 400MHz, CDCl<sub>3</sub>. Aliphatic region (top), aromatic region (bottom)

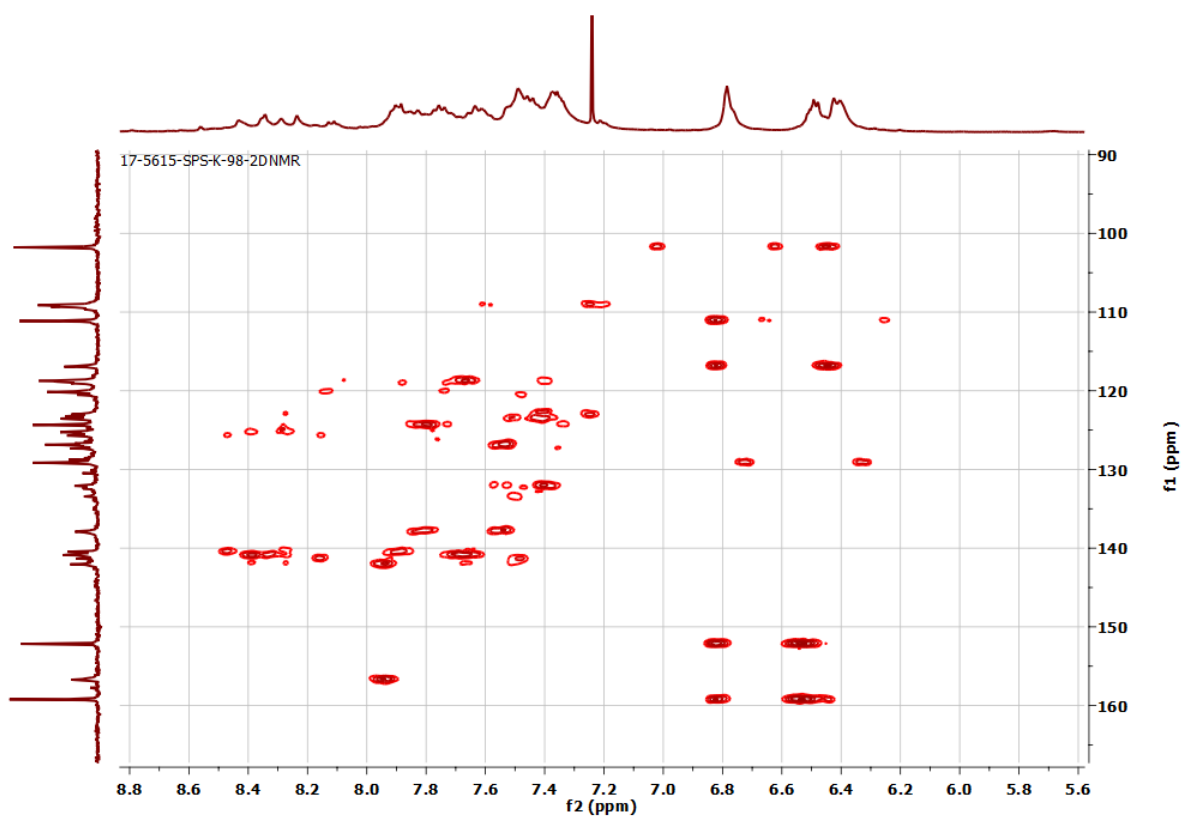
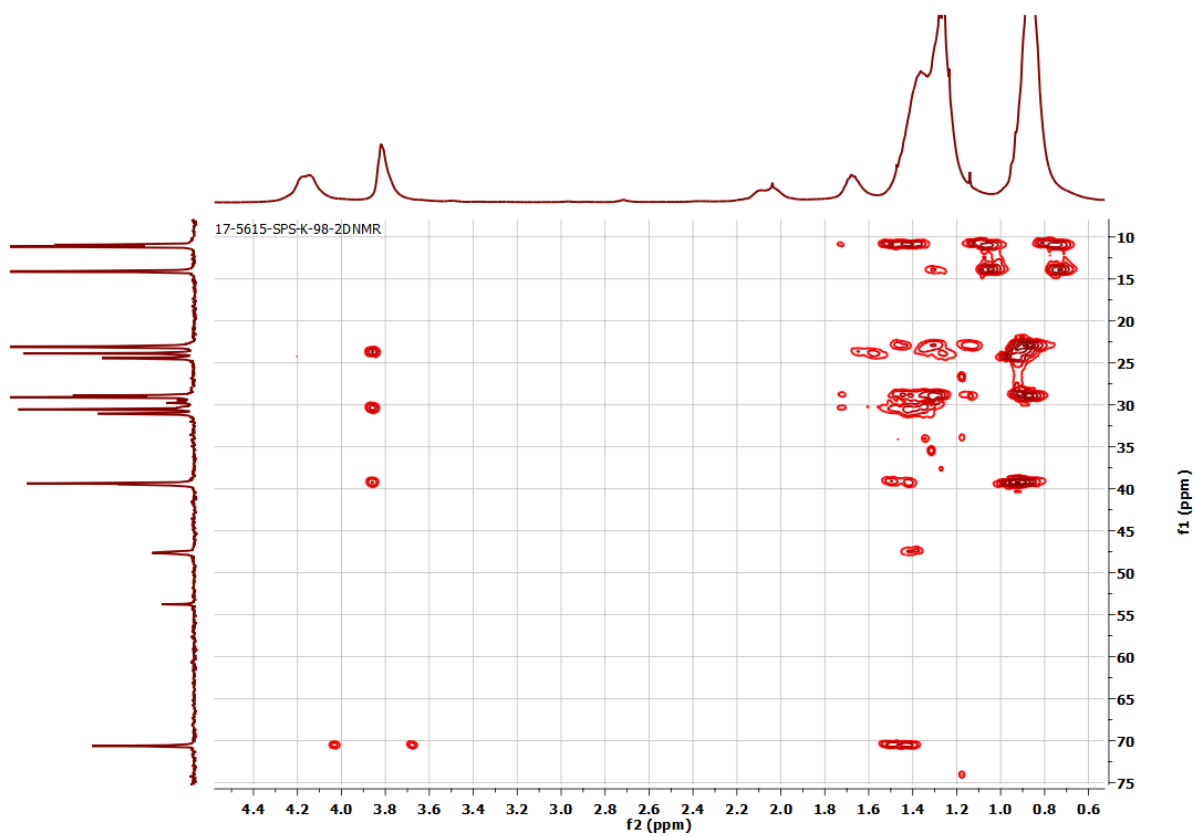


**Figure S32:** Expanded HMBC NMR spectrum of SPS-NR-02, 400MHz,  $\text{CDCl}_3$ . Aliphatic region (top), aromatic region (bottom)

## 6. Mass data:

SPS-OR #29-42 RT: 0.14-0.19 AV: 4 SB: 49 0.32-1.20 NL: 7.79E5  
T: FTMS + p ESI Full ms [200.0000-3000.0000]

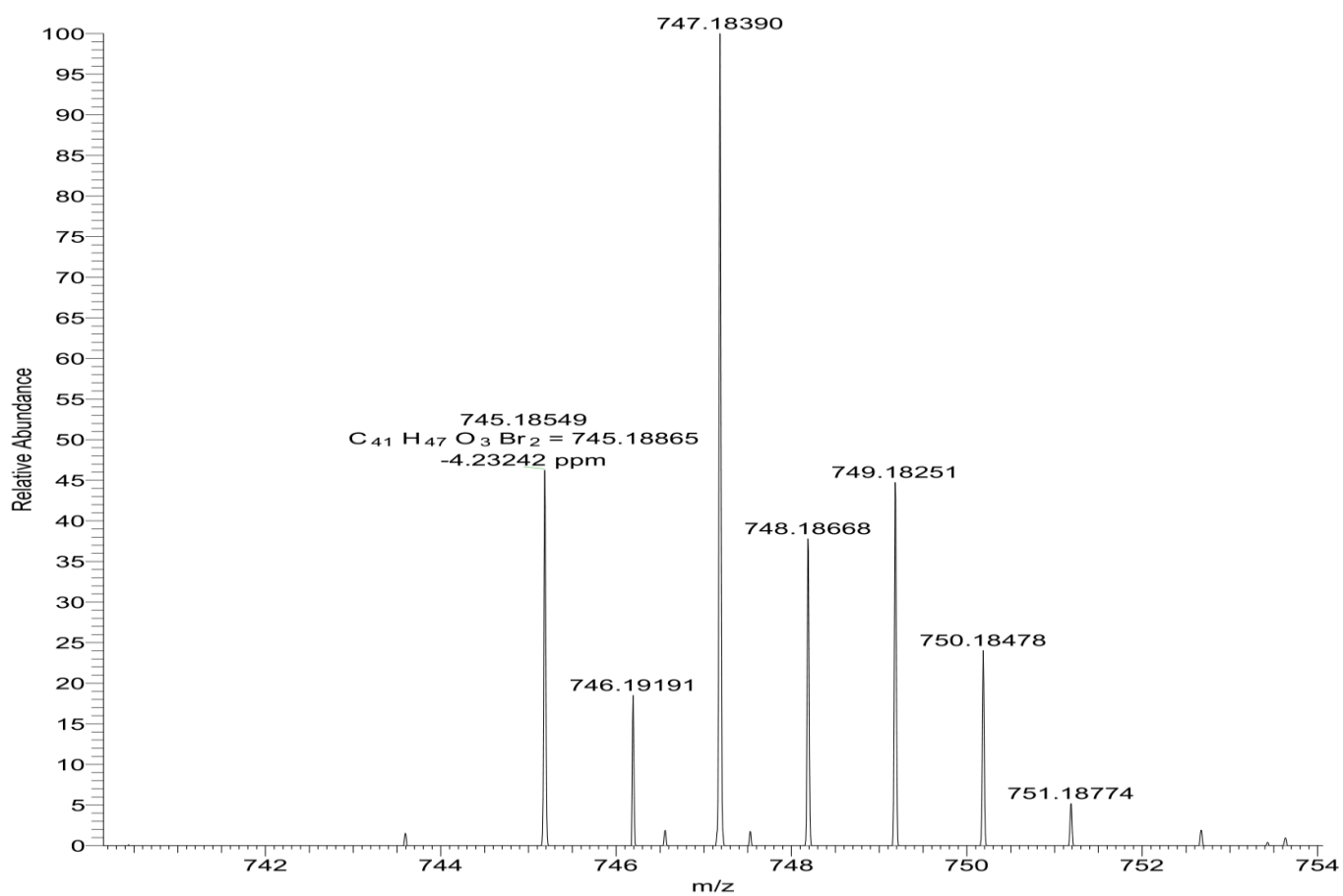


Figure S33: ESI HRMS of SFX-OR.



SPS-BPIN #1-35 RT: 0.01-0.16 AV: 9 SB: 50 0.32-1.20 NL: 6.79E7  
T: FTMS + p ESI Full ms [300.0000-3000.0000]

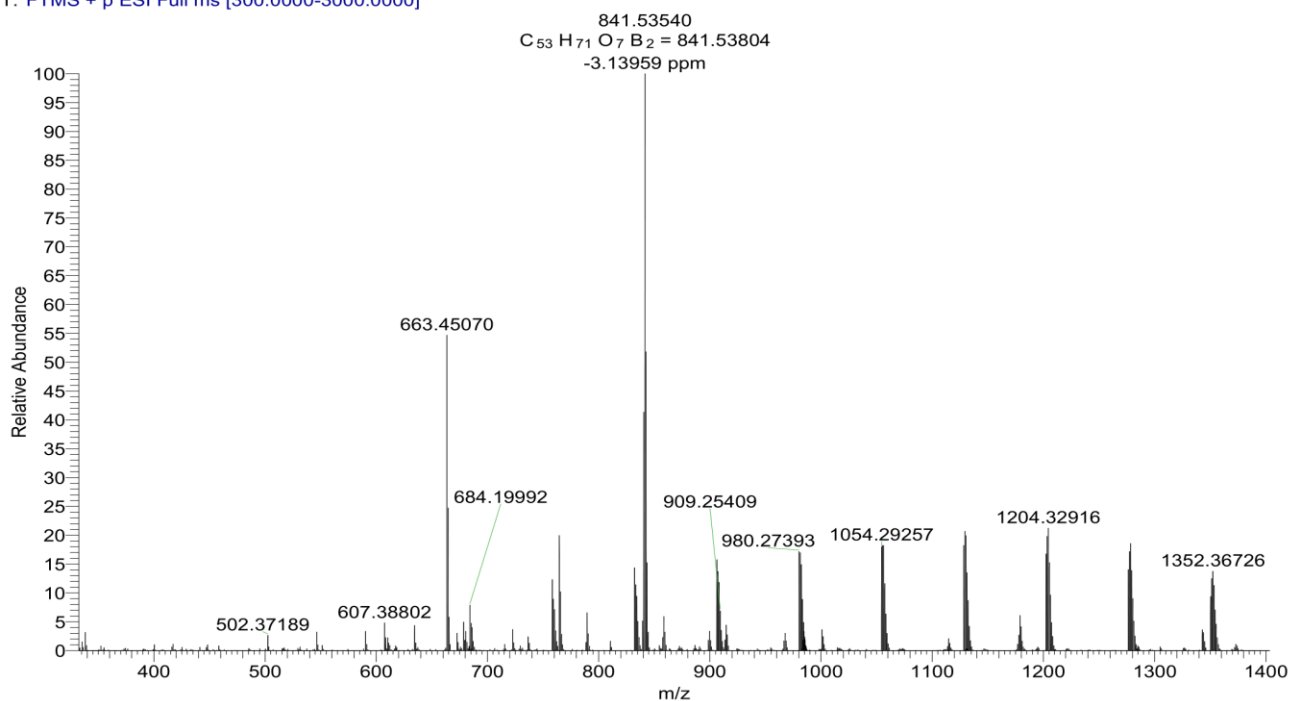


Figure S34: ESI-HRMS of Bpin-SFX.

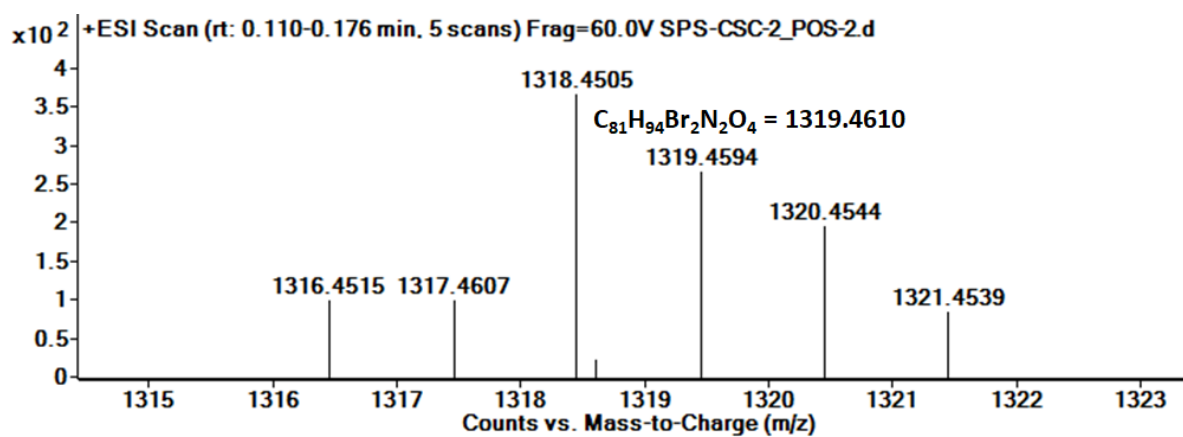
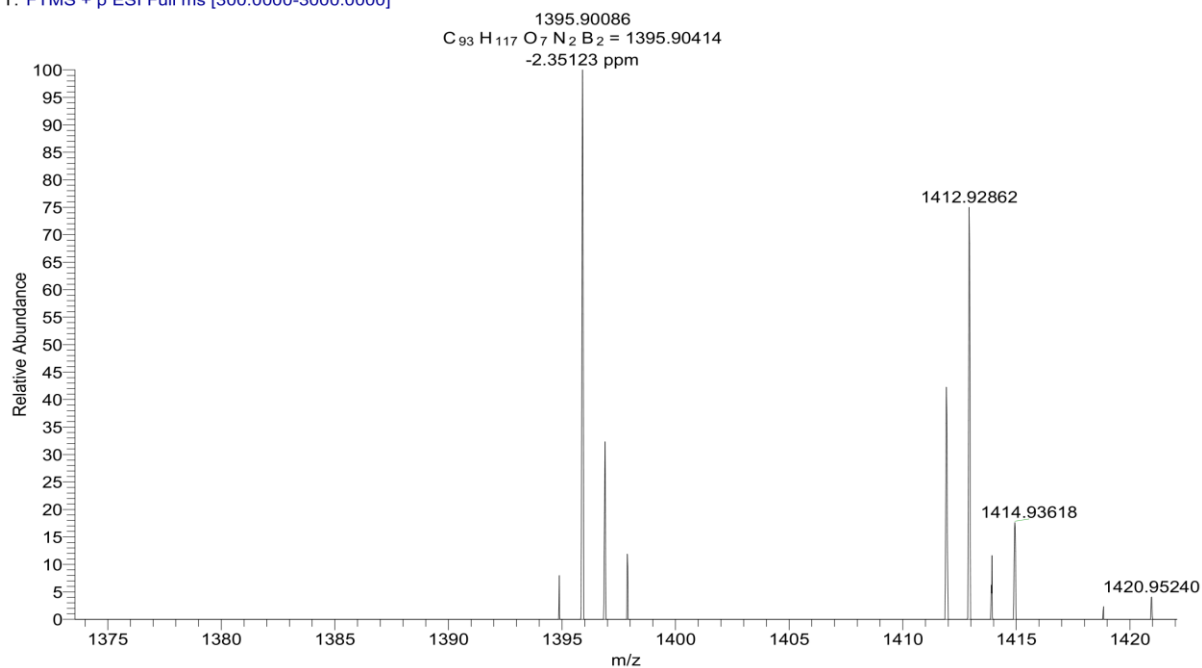
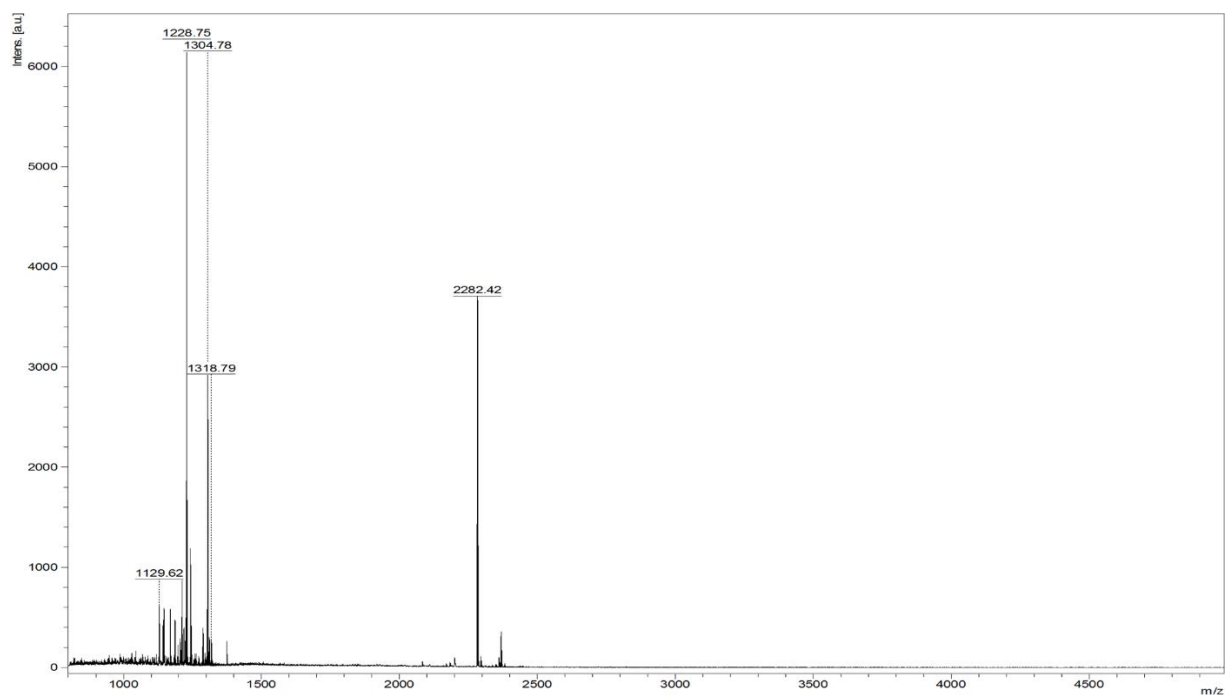


Figure S35: ESI-HRMS of CSC.

SPS-BPIN-CSC #3-24 RT: 0.03-0.10 AV: 5 SB: 48 0.32-1.20 NL: 2.61E5  
T: FTMS + p ESI Full ms [300.0000-3000.0000]



**Figure S36:** ESI-HRMS of Bpin-CSC.



**Figure S37:** MALDI-TOF MS of SPS-NR-02.

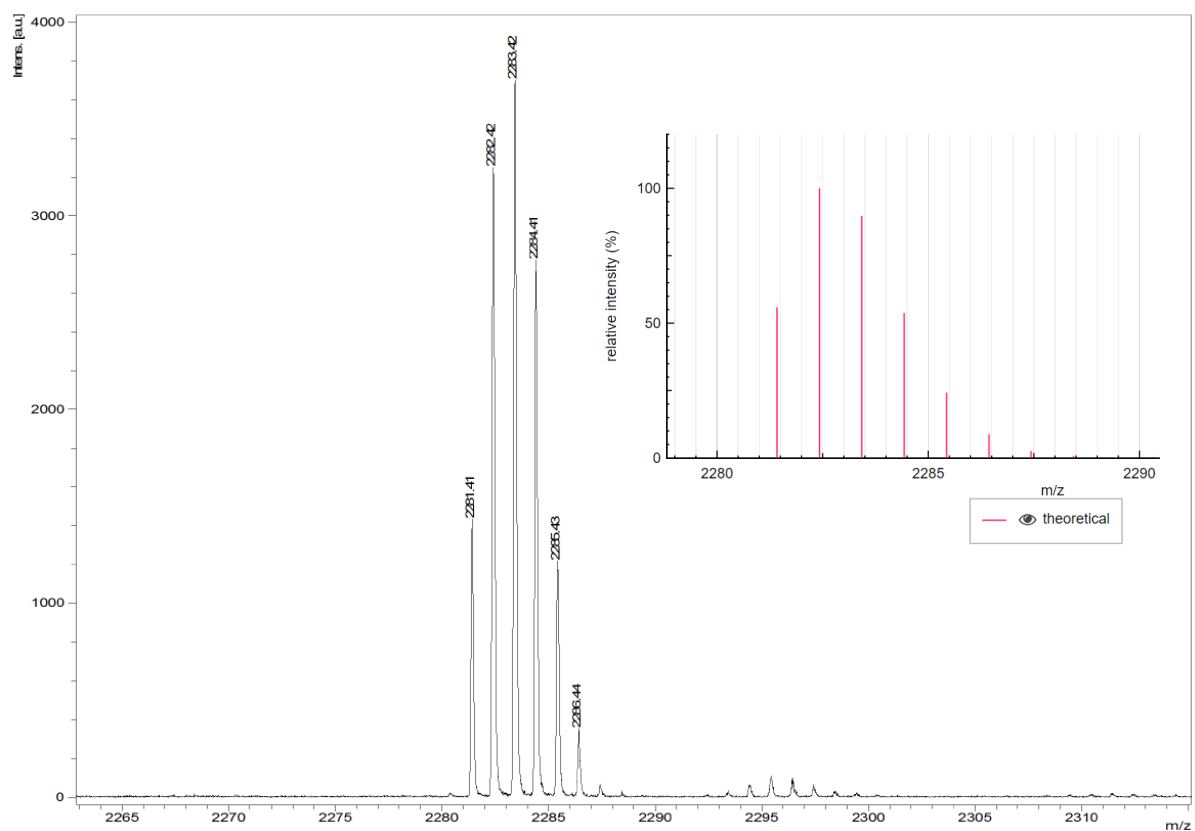
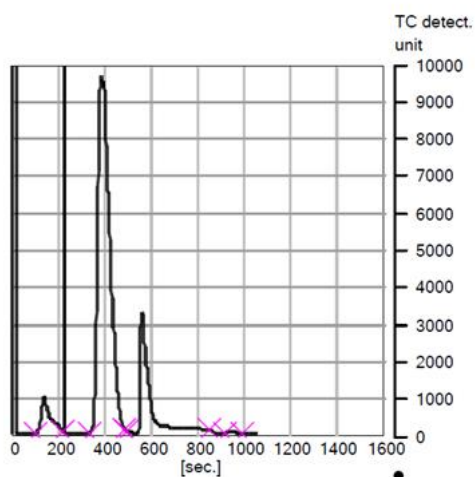


**Figure S38:** MALDI-TOF MS with isotopic distribution for the mass peak of SPS-NR-02 (inset: theoretical simulation of isotopic mass distribution)

analytic functional testing  
 varioMICRO CHNS PV  
 serial number: 15181026

Graphic report

No.	Name	N [%]	C [%]	H [%]	S [%]	Date	Time
27	SPS-NR-02	2.37	85.11	8.137	0.21	07-08-24	09:23 PM



analytic functional testing  
 varioMICRO CHNS PV  
 serial number: 15181026

Graphic report

No.	Name	O [%]	Date	Time
31	SPS-NR-02	4.16	06-08-24	09:22 PM

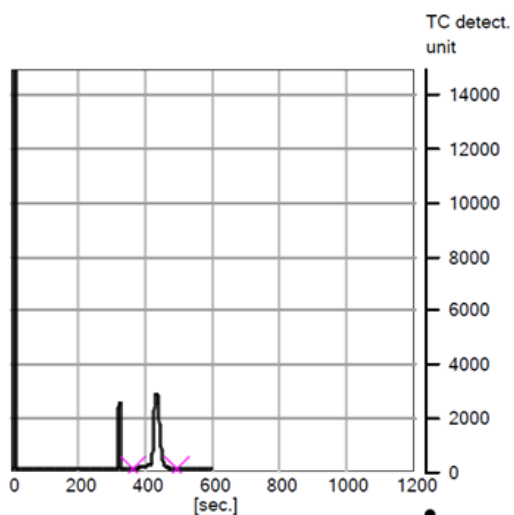


Figure S39: Elemental analysis of SPS-NR-02.

## References:

- [1] B. Yadagiri, T. H. Chowdhury, Y. He, R. Kaneko, A. Islam and S. P. Singh, *Mater. Chem. Front.*, 2021, **19**, 7276-7285.
- [2] G. Sathiyam and P. Sakthivel, *Dyes and Pigments.*, 2017, **143**, 444-454.
- [3] D. B. G. Williams and M. Lawton, *J. Org. Chem.* 2010, **24**, 8351–8354.
- [4] E. M. Espinoza, J. A. Clark, J. Soliman, J. B. Derr, M. Morales and V. I. Vullev, *J. Electrochem. Soc.*, 2019, **5**, H3175-H3187.
- [5] M. J. Frisch, G. W. Trucks, H. B. Schlegel, G. E. Scuseria, M. A. Robb, J. R. Cheeseman, G. Scalmani, V. Barone, G. A. Petersson, H. Nakatsuji, X. Li, M. Caricato, A. V. Marenich, J. Bloino, B. G. Janesko, R. Gomperts, B. Mennucci, H. P. Hratchian, J. V. Ortiz, A. F. Izmaylov, J. L. Sonnenberg, D. Williams-Young, F. Ding, F. Lipparini, F. Egidi, J. Goings, B. Peng, A. Petrone, T. Henderson, D. Ranasinghe, V. G. Zakrzewski, J. Gao, N. Rega, G. Zheng, W. Liang, M. Hada, M. Ehara, K. Toyota, R. Fukuda, J. Hasegawa, M. Ishida, T. Nakajima, Y. Honda, O. Kitao, H. Nakai, T. Vreven, K. Throssell, J. A. Jr. Montgomery, J. E. Peralta, F. Ogliaro, M. J. Bearpark, J. J. Heyd, E. N. Brothers, K. N. Kudin, V. N. Staroverov, T. A. Keith, R. Kobayashi, J. Normand, K. Raghavachari, A. P. Rendell, J. C. Burant, S. S. Iyengar, J. Tomasi, M. Cossi, J. M. Millam, M. Klene, C. Adamo, R. Cammi, J. W. Ochterski, R. L. Martin, K. Morokuma, O. Farkas, J. B. Foresman, D. J. Fox, Gaussian 16, Revision C.01, 2016. Gaussian, Inc., Wallingford CT, 2016 (accessed August 20, 2020).
- [6] J. D. Chai and M. Head-Gordon, *Phys. Chem. Chem. Phys.*, 2008, **44**, 6615-6620.
- [7] S. Bhandari, M. S. Cheung, E. Geva, L. Kronik and B. D. Dunietz, *J. Chem. Theory Comput.*, 2018, **12**, 6287–6294.
- [8] Natural Transition Orbitals (NTOs) Gaussian, Dr. Joaquin Barroso's Blog (2020).
- [9] S. F. Boys and F. J. M. P. Bernardi, *Molecular physics.*, 1970, **4**, 553-566.